The Chromatin Remodelers RSC and ISW1 Display Functional and Chromatin-based Promoter Antagonism

Timothy J. Parnell*, Alisha Schlichter*, Boris G. Wilson, Bradley R. Cairns

Howard Hughes Medical Institute (HHMI), Department of Oncological Sciences, Huntsman Cancer Institute, University of Utah School of Medicine, Salt Lake City, Utah, USA. For correspondence: brad.cairns@hci.utah.edu. *These authors contributed equally.

The authors have no competing interest.

Abstract

ISWI-family chromatin remodelers organize nucleosome arrays, while SWI/SNF-family remodelers (RSC) disorganize and eject nucleosomes, implying an antagonism that is largely unexplored *in vivo*. Here, we describe two independent genetic screens for *rsc* suppressors that yielded mutations in the promoter-focused ISW1a complex, or mutations in the 'basic patch' of histone H4 (an epitope that regulates ISWI activity), strongly supporting RSC-ISW1a antagonism *in vivo*. RSC and ISW1a largely co-localize, and genomic nucleosome studies using *rsc isw1* mutant combinations revealed opposing functions: promoters classified with a nucleosome-deficient region (NDR) gain nucleosome occupancy in *rsc* mutants, but this gain is attenuated in *rsc isw1* double mutants. Furthermore, promoters lacking NDRs have the highest occupancy of both remodelers, consistent with regulation by nucleosome occupancy, and decreased transcription in *rsc* mutants. Taken together, we provide the first genetic and genomic evidence for RSC-ISW1a antagonism, and reveal different mechanisms at two different promoter architectures.

Introduction

Genomic DNA is packaged into chromatin, a dynamic material that exhibits numerous changes in post-translational modifications, composition, and protein interactions. One aspect of chromatin modulation involves the assembly or disassembly of chromatin through active remodeling, which can confer either occlusion or access to the DNA – a process that is associated with virtually all DNA-mediated transactions, including transcription, replication, and repair. Each remodeling action, either assembly or disassembly, is mediated (in part) by specialized ATP-dependent chromatin remodeling complexes (Clapier and Cairns 2009; Vignali et al. 2000; Narlikar, Sundaramoorthy, and Owen-Hughes 2013; Bartholomew 2014).

Certain chromatin remodelers align with these two general categories: those that restrict DNA access by chromatin assembly and organization, and those that promote DNA access by chromatin disassembly and disorganization. This broad separation in function can be partially illustrated by studies of individual chromatin remodelers and their effects on gene expression (Angus-Hill et al. 2001; Vary et al. 2003; Fazzio et al. 2001); in general, remodelers associated with chromatin disassembly promote DNA access and gene expression, while remodelers associated with chromatin organization more often repress gene expression, though there are exceptions to this simplified view (e.g. increased accessibility can promote repressor access to chromatin).

The SWI/SNF family of chromatin remodelers provides a well-studied example of remodelers associated with nucleosome disorganization and/or disassembly. In yeast, the RSC chromatin-remodeling complex is an essential and abundant paralog of the canonical SWI/SNF remodeler (Cairns et al. 1996). The central subunit of RSC, Sth1, is a DNA-dependent ATPase that translocates DNA, pumping DNA around the surface of a nucleosome and effectively mobilizing the nucleosome with respect to the underlying sequence (Saha, Wittmeyer, and Cairns 2002, 2005). This property enables RSC to shift nucleosome positions, as well as completely eject nucleosomes (Clapier and Cairns 2009; Boeger et al. 2004; Dechassa et al. 2010; Lorch, Zhang, and Kornberg 1999). In vivo,

RSC facilitates transcription by all three RNA polymerases, primarily by enabling promoter access (Parnell, Huff, and Cairns 2008). RSC maintains proper promoter chromatin structure, as RSC mutants exhibit alterations in nucleosome occupancy and spacing at promoters (Badis et al. 2008; Hartley and Madhani 2009; Ganguli et al. 2014). RSC activity appears regulated, in part, by the presence of histone modifications (Kasten et al. 2004; Ferreira, Flaus, and Owen-Hughes 2007). RSC contains seven bromodomains on four subunits, implying a key role of acetylation in regulation. Thus, gene activation often involves the recruitment and activation of remodelers such as RSC to act on specific, modified nucleosomes and promote promoter accessibility. The converse of gene activation, silencing, is expected to be the reverse process, where nucleosomes are re-positioned and organized to occlude transcription factor access.

This reconfiguration of chromatin to a less active or repressive state is a function of other chromatin remodelers, including members of the ISWI family. In yeast, these include two highly conserved ATPase paralogs, *ISW1* and *ISW2*, related to the Drosophila '*Imitation SWitch'* (ISWI) protein, which is the catalytic component of multiple chromatin-remodeling complexes with roles in nucleosome assembly and gene repression (Tsukiyama et al. 1999; Vary et al. 2003). Similar to the family of SWI/SNF remodelers, the ISWI family of remodelers uses DNA translocation to mobilize nucleosomes, though ISWI remodelers are typically restricted to movement/sliding only, and not ejection (Clapier and Cairns 2009; Whitehouse et al. 1999). Importantly, ISWI generates regularly spaced nucleosome arrays by 'measuring' the length of DNA linker between nucleosomes, and this property is thought to enable gene repression by ordering nucleosomes into closely spaced regular arrays that can restrict access to DNA (Whitehouse and Tsukiyama 2006; Tirosh, Sigal, and Barkai 2010; Grune et al. 2003; Bartholomew 2014; Gangaraju and Bartholomew 2007).

Studies of remodeler antagonism have been limited. ISW2 function was shown in one study to restrict the binding of the SWI/SNF chromatin remodeler at a target gene in yeast (Tomar et al. 2009). Another study showed antagonistic roles by two alternative assemblies of mammalian SWI/SNF complex (BRG and BRM), where BRM appeared to repress BRG activation functions (Flowers et al. 2009). A third noted attenuation of BRG

activation by the CHD family remodeler Mi-2 (Ramirez-Carrozzi et al. 2006) at a set of target genes. Although notable, none of the prior studies provide a conceptual view of how two remodelers might antagonize one another at a large number of loci, and how antagonism relates to nucleosome occupancy and positioning at co-occupied loci.

Here, we examine remodeler antagonism explicitly, providing the first evidence for an antagonistic relationship between ISWI and RSC. We demonstrate the suppression of growth rate phenotypes and the impact of these remodelers on both transcription and chromatin architecture at a genome-scale. These studies uniquely reveal important activities of these two chromatin remodelers at particular promoter architectures – 'open' and 'closed' – and the requirement for remodeler antagonism for proper regulation.

Results

A genome-wide screen for null suppressors of *rsc7*Δ

Rsc7 is a non-essential subunit of the RSC complex that is required for growth at elevated temperatures and for full growth under particular conditions (Wilson et al. 2006). We previously used a synthetic genetic array (SGA) screen (Tong et al. 2001) to identify genes that induced lethality in combination with *rsc7*Δ (Wilson et al. 2006). We again employed the SGA array to screen for genes whose null mutation would allow for growth of *rsc7*Δ at an otherwise non-permissive temperature.

To accomplish this, a strain containing *rsc7*Δ was crossed to a haploid deletion library comprised of 4,700 strains, each bearing a deletion in a single nonessential gene (SGA array). Double mutants were isolated and screened for growth at a restrictive temperature. Four viable combinations were obtained, including combinations of *rsc7*Δ with *rpl20b*Δ, *lsm7*Δ, *bud31*Δ, or *isw1*Δ (Figure 1A, Figure 2C (33ºC), and data not shown). The first three genes are associated with various ribonucleoprotein complexes, including ribosomes and snRNPs, which may represent interesting pathways that involve RSC function. However, the identification of *isw1*Δ was particularly intriguing, as it suggested a possible antagonistic relationship between ISWI complex(es) and RSC. Suppression

was linked to *isw1*Δ, as the *rsc7*Δ temperature sensitivity returned with the introduction of a wild type copy of *ISW1* on a plasmid (Figure 1A). The specificity of this observation is notable, as virtually all combinations of *rsc7*Δ with mutations in other chromatin-related genes typically resulted in lethality (Wilson et al. 2006); thus, *isw1*Δ was the sole suppressing mutation with a chromatin/transcription function isolated in our genome-wide format.

A screen for suppressors of *RSC2* mutations yields suppressing mutations in Histone H3 and H4

The suppression relationship between RSC and *ISW1* was further strengthened through a second independent genetic screen involving *RSC2*. The Rsc1 and Rsc2 proteins are two homologous, mutually exclusive subunits of RSC that define two distinct RSC sub-complexes (Cairns et al. 1999). Loss of either separately confers distinct phenotypes, while loss of both is lethal, suggesting both unique nonessential and redundant essential functions within the complex (Cairns et al. 1999). Rsc1 and Rsc2 share the same domain structure, which consists of one nonessential and one essential bromodomain (Cairns et al. 1999), a BAH domain that binds histone H3 (Tsankov et al. 2011), and an AT hook (Cairns et al. 1999). We previously isolated mutant alleles in the BAH domain of Rsc2, including *rsc2-V457M* and *rsc2-D461G*, that confer temperature sensitivity in *rsc1*Δ strains (Schlichter and Cairns 2005).

To identify whether histone mutations might suppress RSC mutations, we employed a histone mutagenesis screen. We integrated the *rsc2-V457M* allele into a *rsc1*Δ strain bearing histone H3-H4 deletions (*hht1-hhf1*Δ and *hht2-hhf2*Δ) that was covered by a *URA3*-marked plasmid bearing wild type histones, *HHT2-HHF2*. We then introduced *TRP1*-marked plasmids containing hydroxylamine mutagenized *HHT2-HHF2* genes, and screened for suppression of the temperature sensitivity phenotype upon loss of the wild type histone plasmid (using 5-FOA negative selection). From 20,000 transformants screened, we isolated seventeen suppressors that were verified by isolating and retransforming the plasmid containing the histone mutation. Of these, most contained single mutations: eight had either H3 A7V or H3 A7T mutations, seven had an H3 T6I

mutation, and one bore an H3 G33V mutation. However, one mutant bore an H4 RH17,18CY double mutation (Figure 1B). All of these histone mutations were also tested for suppression of other temperature sensitive RSC alleles, including *rsc2-D461G*, *rsc2-Y337H*, and *rsc4-2*, and each was suppressed (data not shown), suggesting that these mutations generally suppress RSC defects, and not a specific defect of *rsc2-V457M*. We focused on the H4 RH17,18CY mutant for subsequent studies as it caused the most robust suppression (Figure 1B).

The H4 RH17,18CY mutations are adjacent to H4 K16, a residue whose acetylation serves as a mark for active chromatin (Millar, Kurdistani, and Grunstein 2004). As RSC contains several bromodomains and may be regulated by histone acetylation (reviewed in (Josling et al. 2012), we considered whether loss of H4 K16 acetylation may underlie the suppression. However, no H4 K16 acetylation was detected by western blot in the H4 RH17,18CY mutant, but this could either be the result of loss of acetylation or failure of the antibody to recognize the mutated epitope. We therefore combined *rsc2-V457M* with H4 K16Q, H4 K16R, and H4 K16G mutants to determine if loss of K16 acetylation was responsible for the suppression. However, combining these mutants resulted in a slight synthetic sickness instead of suppression (Figure 1C), ruling out this simple model.

Notably, the H4 RH17,18CY mutations define the center of a region of the H4 tail referred to as the 'basic patch', an epitope of known importance for the binding and activity of several chromatin-modifying factors including Isw1, Sir3, and Dot1 (Clapier, Nightingale, and Becker 2002; Fazzio, Gelbart, and Tsukiyama 2005; Fingerman, Li, and Briggs 2007; Altaf et al. 2007; Wang et al. 2013). To test if the suppression by the basic patch mutation was due to an inability of Dot1 to bind or methylate H3K79, we combined *rsc2-V457M* with either an H3 K79A mutation or *dot1* null mutant. However, we observed no effect with the H3 K79A mutation (Figure 1C), and the combination with *dot1*Δ resulted in synthetic sickness (Figure 1 Supplement 1). Additionally, combination with a *sir3*Δ failed to suppress (Figure 1 Supplement 1). Taken together, our results point strongly to *ISW1* as the most likely candidate for RSC mutant suppression, tested further below.

Loss of *ISW1* suppresses RSC mutations

The results of these two genetic screens strongly suggested a functional antagonism between RSC and Isw1. To directly test *isw1* mutant suppression of *rsc2* alleles, we combined *rsc2-V457M* or *rsc2-D461G* with *isw1*Δ and observed partial suppression of temperature sensitivity and a set of phenotypes associated with the drugs benomyl and formamide (Figure 2A) as well as 6-azauracil (6AU) and mycophenolic acid (MPA) (Figure 2B). Growth suppression of the double mutant was lost when *ISW1* was restored through plasmid transformation. Suppression requires a loss of ISW1 catalytic function, as *rsc2* suppression is observed in a strain bearing a mutation in the catalytic site (K227A) of ISW1 (Figure 2 Supplement 1A). Furthermore, when we combined *rsc2-V457M* with both *isw1*Δ and H4 RH17,18CY, no enhanced suppression was observed (data not shown), suggesting that they act through the same pathway. We also directly tested whether the *ISWI* paralog, *ISW2*, might also suppress *rsc2* alleles. Combining the *isw2*Δ mutation with *rsc2-V457M* or *rsc2-D461G* did not confer suppression of the temperature growth defect, although some partial suppression of other phenotypes was observed (Figure 2 Supplement 1B). We also did not see additional suppression when *isw1*Δ and *isw2*Δ were combined (data not shown). We therefore conclude that the *rsc2* mutation suppression is due primarily to the loss of Isw1 activity, with minimal contributions from of loss Isw2 activity.

We next asked whether *isw1*Δ suppression was specific to *rsc2* and *rsc7* mutations or could extend more generally to RSC mutations. To test this, we combined *isw1*Δ with two additional RSC mutations in separate subunits, *rsc3-3* and *rsc4-2*. The *isw1*Δ allele suppressed both RSC mutations tested (Figure 2C), with suppression of *rsc4-2* particularly robust and greater than *rsc2* mutants (Figure 2C, YPD 38ºC panel). We also tested whether *isw1*Δ could suppress phenotypes associated with loss of SWI/SNF function. Combining *isw1*Δ with *snf2*Δ did not allow growth on galactose or raffinose carbon sources, or growth on media containing hydroxyurea (Figure 2C), demonstrating specificity for RSC. Together, these results are consistent with a specific, antagonistic relationship between RSC and *ISW1*.

Suppression of *rsc2* by *isw1*Δ is specific to the ISW1a complex.

Isw1 is the ATPase for two distinct remodeling complexes, ISW1a and ISW1b (Vary et al. 2003). The ISW1a form contains Ioc3, associates with particular gene promoters, and is implicated in repression by positioning nucleosomes into regularly spaced arrays (Gangaraju and Bartholomew 2007; Yamada et al. 2011). ISW1b contains Ioc2 and Ioc4, associates with coding regions, plays a greater role in transcription elongation and termination, and does not regularly space nucleosomes. (Morillon et al. 2003; Gangaraju and Bartholomew 2007; Vary et al. 2003). To determine which form of the ISW1 complex is responsible for the suppression of *rsc2*, we combined *rsc2-V457M* with *ioc2*Δ, *ioc3*Δ, or *ioc4*Δ. Surprisingly, synthetic lethality, and not suppression, was observed when *rsc2-V457M* was combined with either *ioc2*Δ or *ioc4*Δ (Figure 3A). In contrast, combining *rsc2-V457M* with *ioc3*Δ resulted in partial suppression of *rsc2* phenotypes (Figure 3B). Notably, *ioc3*Δ potently suppressed *rsc4-2* (Figure 3C) and partially suppressed conditional *rsc1* mutations (Figure 3 Supplement 1). Together, these results strongly implicate the loss of Isw1a complex function in *rsc* suppression.

Loss of *isw1*Δ reduces the reliance of RSC on certain histone modifications

Our prior work revealed moderate *rsc2* suppression with increased H3K4me3 (via hyperactive *SET1* alleles), and conversely, synthetic lethality with *rsc2 set1*Δ combinations, suggesting that H3K4me3 either promotes or partially bypasses RSC activity (Schlichter and Cairns 2005). However, as ISWI activity is affected by H3K4me and Set1 function (Santos-Rosa et al. 2003), an alternative hypothesis is that H3K4me affects RSC indirectly through the alteration of Isw1 activity. To test this, we combined *rsc2-V457M* or *rsc2-D461G* with *set1*Δ, in the absence or presence of *ISW1* or *IOC3*. Interestingly, either *isw1*Δ or *ioc3*Δ can suppress the *rsc2 set1*Δ lethality (Figure 3 Supplement 2). We also find that there is no additional suppression of *rsc2* temperature sensitivity by combining *SET1* hyperactive mutations and *isw1*Δ, and that *isw1*Δ can still suppress *rsc2* phenotypes in an H3 K4A mutant (data not shown). These results suggest that suppression by loss of Isw1a is epistatic to the effects of Set1 loss and can overcome the reliance of RSC on H3K4 methylation.

As RSC activity is known to also be promoted by histone acetylation (e.g. H3K14ac; (Ferreira, Flaus, and Owen-Hughes 2007; Kasten et al. 2004; Carey, Li, and Workman 2006), we therefore tested whether loss of Isw1 would reduce the reliance of RSC on H3K14ac. *GCN5* is a histone acetyltransferase responsible for much of the H3K14ac *in vivo* (Howe et al. 2001; Johnsson et al. 2009), and loss of *GCN5* is lethal in combination with several RSC mutations, including *rsc2*Δ (Cairns et al. 1999; Kasten et al. 2004). We found *isw1*Δ suppressed the lethality of *rsc2*Δ *gcn5*Δ mutations (Figure 3 Supplement 2). These results suggest that removing the chromatin remodeler that antagonizes RSC, notably Isw1a, reduces the need for RSC activation though acetylation.

RSC and ISWI co-occupy many genomic locations

The genetic relationships identified above prompted us to investigate the spatial relationship between RSC and ISW1a. We therefore determined the occupancy of both of these chromatin remodelers by chromatin immunoprecipitation (ChIP), using the RSC subunit Rsc8 and the ISW1 subunit Ioc3, both tagged with C-terminal Myc epitope tags. We chose the Rsc8 subunit of RSC because it exists as a dimer in the RSC complex, minimizing the low ChIP efficiency observed with chromatin remodelers (Yen et al. 2012; Whitehouse et al. 2007; Parnell, Huff, and Cairns 2008). We analyzed the immunoprecipitated DNA first by hybridization to high-resolution genome-wide microarrays (244K probes, ~50 bp resolution) and subsequently high-throughput sequencing.

RSC occupancy was scored across gene promoters (-800 to +800 bp), and promoters were then sorted into six clusters using a k-means algorithm to visualize those with and without enrichment (Figure 4A). Using the mean occupancy at the transcription start site (TSS, ±250 bp), 43% of promoters (2274 out of 5337) had RSC enrichment corresponding to a False Discovery Rate (FDR) of less than 1%. We also found RSC was highly enriched at all non-coding RNA genes, including tRNA genes, as reported previously (Ng et al. 2002). Notably, we find RSC highly enriched at virtually all centromeres (Figure 4B), a localization not previously reported.

In comparison to RSC, the Ioc3 enrichment was less robust, perhaps reflecting a difference in chromatin association or difficulty in capturing complexes. We identified 137 or 230 Pol II promoters at an FDR of 1% or 5%, respectively. Strikingly, 224 of these latter promoters also pass the 1% threshold for RSC enrichment. Visual comparison of the enrichment pattern (log2 fold ChIP/Input) across all Pol II promoters reveals a high degree of overlap (Figure 4A), while a pairwise plot between the RSC and ISWI mean fold-enrichment values at the TSS shows a positive correlation (r=0.6 ; Figure 4C). This enrichment also extends beyond Pol II promoters, as we observed high ISW1a occupancy at both ncRNA and tRNA genes (Figure 4B). We did not observe significant enrichment of ISW1 at centromeres, although we note that ISW2 is enriched at centromeres (Zentner and Henikoff 2013), which may provide any requisite ISWI function at these loci. These results support the notion that RSC and ISW1a share a spatial (though perhaps not temporal) occupancy at particular genes.

To extend these results, we repeated Rsc8, Ioc3, and Sth1 (the ATPase subunit of RSC) ChIP using micrococcal-nuclease digested chromatin analyzed by paired-end sequencing. We compared the log2 fold enrichment values obtained from both microarray and sequencing technologies (Figure 4 Supplement 1). Despite the differences in resolution and sensitivity between these methods, we observed strong correlations between our microarray and sequencing results.

Transcription-based suppression of *rsc2* by *isw1*

Since a complete loss of RSC function results in a cessation of all transcription from all three polymerases (Parnell, Huff, and Cairns 2008), a weaker, viable mutation (such as those in *rsc2*) may result simply in an attenuation of transcription of many or all genes, leading to a general phenotype such as temperature sensitivity. This transcription attenuation, as well as any suppression by ISWI, should be evident by expression analysis. To determine whether this suppression is global in nature or restricted to a subset of genes, we performed a HybMap analysis on a sampling of genes in the genome. The HybMap technique measures both sense and antisense RNA levels across a genome (Dutrow et al. 2008), providing results that are comparable to RNA-Seq (Ni et al. 2010).

The advantage of this technique is the direct use of total RNA (enabling the detection of transcripts lacking polyA) without RNA labeling and/or amplification protocols to obtain absolute expression levels. Although the format restricted our array to 649 genes, it included a large fraction of genes occupied by RSC (84%), both RSC and ISW1 (9%), or unoccupied (16%), using an FDR threshold of 1%. We performed this analysis on *rsc2-V457M*, *isw1*Δ, *ioc3*Δ, *rsc2-V457M isw1*Δ, and *rsc2-V457M ioc3*Δ strains and compared them to wild type.

Consistent with the general requirement of RSC function for transcription (Parnell, Huff, and Cairns 2008), the mean expression of both coding and non-coding genes (but not tRNAs) was reduced almost 2-fold following the loss of RSC (Figure 4D). Interestingly, individual *ioc3* or *isw1* mutants also lowered mean expression, but with less magnitude. However, neither the *rsc2 ioc3* nor the *rsc2 isw1* double mutants generally suppressed the *rsc2* effect by restoring global gene expression. Furthermore, we saw little change among tRNA genes from any genotype, and no measureable change in antisense transcription levels (data not shown). We also did not observe general, aberrant transcription from promoters as reported previously in a *rsc3* mutant (van Bakel et al. 2013). These results suggest that the suppression of RSC phenotypes is not due to a global effect on gene expression, but rather due to an effect at a subset of genes. To see if such genes could be identified from our sampling, we selected genes whose expression was at least partially restored by combining *rsc2* with *isw1* or *ioc3* mutations. This analysis revealed 20 genes (Figure 4 Supplement 2), which included genes for ribosome function, snoRNA genes, and several essential genes. It is likely that the combined modest change in expression at these and other genes are responsible for the suppression relationship observed.

ISW1 mutations suppress nucleosomal shifts in RSC mutants

Since RSC and ISW1 are both chromatin remodelers, the most important test for antagonism involves examining whether mutations in *ISW1* could suppress the effects of nucleosomal changes due to the loss of RSC function. Loss of RSC results in a gain of nucleosome occupancy at the nucleosome depleted region (NDR) commonly found near the TSS of genes (Parnell, Huff, and Cairns 2008; Hartley and Madhani 2009; Badis et al.

2008; Ganguli et al. 2014). We therefore constructed strains that included the *sth1*^{td} degron allele in combination with an *isw1*Δ allele. Implementation of the *sth1*^{td} allele allows for precise, inducible destruction of the catalytic subunit of RSC, thus abrogating all RSC catalytic function – which we subsequently term 'rscΔ' in figures and text. We chose to use both the RSC and *isw1* null alleles to maximize the nucleosomal effects due to the loss of catalytic activity in a manner that mutations in regulatory subunits may not. Mono-nucleosomal DNA was isolated from these yeast strains after inducing the degron allele for 2 hours and analyzed by both high-resolution microarray (rscΔ and *isw1*Δ) and paired-end sequencing (rscΔ only). As a reference we also analyzed mono-nucleosomal DNA from control strains that cannot degrade Sth1 protein. To analyze the chromatin structure around the TSS, we generated nucleosome profiles around the TSS for every promoter by scoring the nucleosomal occupancy for rscΔ and RSC strains. Promoters were organized into clusters based on their rscΔ/RSC ratio profile using a k-means algorithm (Figure 5A). For each cluster, the mean nucleosome profile of both strains was then generated (Figure 5B). (We note that the clusters in Figure 5 bear no relationship to the clustering analysis in Figure 4, which instead shows similarity in loci occupied by RSC or ISWI).

The aggregate nucleosome profiles of wild type (blue line, Figure 5B) confirmed published observations (Yuan et al. 2005; Lee et al. 2007; Whitehouse et al. 2007), showing a clear NDR flanked by positioned nucleosomes (termed -1 and +1), and phased positioned nucleosomes within the proximal coding region. The loss of RSC (Figure 5A and Figure 5B) resulted in two major categories: 1) clusters 1-4 all share strong changes in nucleosome positioning following the loss of RSC, and 2) clusters 5 and 6 show a weak response to the loss of RSC. Closer examination revealed further differences in each category. For example, the cluster 1 rscΔ profile shows a dramatic gain in nucleosome occupancy over the NDR at the expense of the +1 nucleosome relative to the control RSC profile, consistent with prior work (see Discussion). There is also a clear 'leftward' shift in nucleosome positions over the body of the gene, towards the NDR. This nucleosome shift is particularly prominent in clusters 3 and 4, while the NDR is filled in to a lesser extent and the +1 nucleosome peak is not as depleted (compared to cluster 1). To confirm that these effects were not due to limitations in the sensitivity and

resolution of microarray analyses, the nucleosome profiles from the microarray data were directly compared to those from the sequencing analysis (Figure 5 Supplement 1). Nucleosome profiles of the same clusters show remarkable similarity between those derived from array and sequence, validating our approaches and conclusions. Taken together, the filling of the NDR and a strong 'leftward' shift of the +1 nucleosome toward the NDR are consistent features that follow loss of RSC function.

We next examined the impact due to the loss of *ISW1* (Figure 5D). Loss of *ISW1* results in modest nucleosomal changes, most notably within the promoter proximal 5' coding region, either as changes in density or phasing, and minimal impact at the NDR. While loss of *ISW1* alone has been shown to result in nucleosomal shifts towards the TSS (Tirosh, Sigal, and Barkai 2010; Yen et al. 2012; van Bakel et al. 2013), these shifts, discernable in cluster 3, are much smaller and more restricted than those generated by the loss of RSC (compare Figures 5B and 5D). Importantly, in the double mutant (Figure 5C) the nucleosomal profiles are more similar to wild type than rscΔ alone. Notably, the NDRs are not as filled and the shifts towards the TSS are not as severe. Taken together, these results provide considerable support for an antagonistic relationship between RSC and ISW1, especially regarding the positioning and phasing of nucleosomes over the promoter-proximal coding region of the gene.

RSC loss impacts nucleosome structure at Structured/Open promoters more than Unstructured/Closed promoters

Above we showed that nucleosome architecture at clusters 1-4 show a strong response to RSC loss whereas clusters 5 and 6 show apparently limited changes. Clusters 1-4 display a prototypical promoter nucleosomal architecture (-1, NDR, and +1 nucleosome). In contrast, clusters 5 and 6 lack this stereotypical organization; here, RSC and/or ISW1a may indeed impact nucleosome occupancy and/or positioning, but the effect may be obscured due to architectural heterogeneity. Notably, these two types of architectures have previously been designated as open (or structured) versus closed (or unstructured), and have been largely correlated with either constitutive or highly regulated gene types, respectively (Tirosh and Barkai 2008; Cairns 2009). We verified these classifications by

plotting the mean nucleosome prediction (Segal et al. 2006) for each of these clusters (Figure 5 Supplement 1B). While the predictive power for individual nucleosome positions was weak, the algorithm predicted the depth and breadth of NDRs fairly accurately. The strongly responsive clusters 1-4 had a well-defined NDR prediction, matching the observed profile, while the weakly-responsive clusters 5 and 6 showed a broad, shallow NDR. Since nucleosome phasing is, in part, determined by how well the -1 and +1 nucleosomes are positioned flanking the NDR, this result matches well with the general lack of consistent phasing across cluster 5 and 6 gene bodies. Interestingly, cluster 3 does not show as strong a predictive NDR as clusters 1, 2, and 4, which may partly explain why this cluster shows nucleosomal shifts in both *isw1*Δ and rscΔ and weak suppression in the double mutant. Taken together, structured/open promoters show the strongest response to RSC loss, whereas unstructured/closed promoters lack a strong response – though we note that the lack of a uniform structure may obscure the response (see Discussion).

Given the strong impact on chromatin structure at open/structured promoters versus the closed/unstructured promoters, we next examined how the loss of RSC might impact the transcription of these classes. Using our HybMap RNA expression data as a proxy for transcriptional impact, we scored genes from each category for expression. We note, however, that the differences between the HybMap and nucleosome experiments in several parameters, e.g. RSC mutation vs. depletion, time points, and representation among clusters (see Figure 6 Supplement 1A), place limitations on these comparisons. Nevertheless, while all promoter classes showed reduced gene expression in *rsc2* mutants (consistent with Figure 4D), cluster 2 and especially clusters 5 and 6 (the two 'closed' promoter clusters) were most severely negatively impacted (Figure 6A). The inclusion of cluster 2 with clusters 5 and 6 is intriguing; however, it is also the only structured cluster to exhibit significant nucleosome occupancy gain over the body of the gene in rscΔ, which is likely related to the reduction in transcription. These impacts are not simply correlated with the level of gene expression, as the distribution of wild type expression values between clusters is highly consistent (Figure 6 Supplement 1). Similar to what we observed previously, the *isw1*Δ mutants showed little impact on the bulk expression of these genes (Figure 6A). We also examined the chromatin structure of the 17 Pol II

transcribed genes where ISW1a loss provided significant suppression of *rsc2*Δ (Figure 4 Supplement 2). However, the moderate resolution provided by the microarray format limited the fine mapping of nucleosomes, preventing our ability to identify nucleosomes that might be directly responsible for suppression (data not shown). These 17 genes partitioned slightly more to closed (nine genes) than the more common open promoter structures (eight genes). Together, these results suggest that while the clearest effects on nucleosome positioning (restoration in *isw1*Δ) are seen with 'open' promoters, the largest effects on transcription are more closely associated with 'closed' promoters (Figure 6A).

Unstructured/closed promoters have the highest RSC occupancy

We next addressed the relationship between RSC occupancy and promoter architecture (open versus closed promoters). Here, we plotted the mean occupancy profile for both Rsc8 and Ioc3 (Figure 6B and Figure 6 Supplement 2) across the promoter for each of the six clusters identified in Figure 5. One might expect that genes with a strong response in regard to nucleosome positioning would have high RSC occupancy. Somewhat surprisingly, we found the opposite result. Clusters 5 and especially 6 had the highest mean occupancy of both RSC and ISW1a. We also examined other chromatin remodeler occupancies, including SWI/SNF (this study), Isw2 (Zentner and Henikoff 2013), and Chd1 (Zentner and Henikoff 2013). Notably, Isw2 and SWI/SNF occupancy displayed higher occupancy in cluster 6, while Chd1 was more equally distributed among the clusters. Interestingly, histone H2AZ demonstrated an inverse relationship, as clusters 5 and 6 bore the least H2AZ. Considering that these two gene clusters have the highest occupancy of chromatin remodelers, we next asked whether these genes also exhibited high histone turnover. We plotted the mean profile of measured histone turnover rate (Rufiange et al. 2007) over the six gene clusters, and found that the degree of histone turnover correlated well with remodeler occupancy, with cluster 6 having the highest turnover, particularly around and upstream of the TSS (Figure 6C). Thus, unstructured/closed promoters have the highest remodeler occupancies and the highest turnover.

Together, these observations coalesce around the idea that these gene clusters identified in Figure 5, based solely on the impact of RSC remodeler loss, also broadly segregate genes into two distinct types of promoter architectures: open (structured) promoters, and closed (unstructured). The gene clusters with the greatest measurable impact on chromatin organization due to RSC loss, groups 1-4, represent the open promoters, whereas groups 5 and 6 represent closed promoters, which collectively lack a distinctive organization and therefore a measurable impact. These promoter architectures matched well with the predictions of remodeler occupancy and histone turnover (Cairns 2009; Tirosh and Barkai 2008). These architectures are also predicted to correlate with specific DNA sequence characteristics and nucleosome composition. For example, open promoters typically contain nucleosome exclusion sequences clustered with binding sites for factors that may help exclude or reposition nucleosomes (Hartley and Madhani 2009; Badis et al. 2008; Segal et al. 2006). To verify these, we scored promoters for the presence of TATA, Reb1, and Rsc3 binding sites, as well as the number of AAAAA sequences, which antagonize nucleosome formation (Segal and Widom 2009; Kaplan et al. 2009). We then calculated the statistical enrichment of these sequence attributes for both structured (clusters 1-4) and unstructured (clusters 5-6) genes over background by random permutation analysis. We found that clusters 1-4 showed statistically significant enrichments for Reb1 and Rsc3 binding sites and AAAAA sequences, while closed promoters showed an enrichment of TATA binding sites, matching the predictions (Figure 6D). Importantly, it is unstructured/closed and TATA-rich promoters that have been shown previously to mostly rely on chromatin modifiers and remodelers for their activation (Raser and O'Shea 2004; Musladin et al. 2014). As developed in the Discussion, we believe our results, combined with others, argue for two different modes of impact of RSC and other remodelers at the two promoter types: open and closed (Figure 7).

Discussion

Chromatin remodelers represent a set of complexes with different functional roles; some remodelers are primarily involved in transcriptional activation, while others are more

435 dedicated to chromatin assembly and/or transcriptional repression. Here, we describe an
436 antagonistic relationship between two such chromatin remodelers, RSC and ISW1,
437 through a combination of genetics, gene expression, and genome-wide nucleosome
438 positioning studies. At genes, RSC is primarily utilized for gene activation, providing this
439 function, at least in part, by establishing or maintaining the NDR structure at promoters.
440 We find that this function is partly counteracted by Isw1 activity, which re-positions
441 nucleosomes to "fill in" the NDR and positions nucleosomes over *cis* regulatory
442 sequences. While there are other remodelers that also act at promoters, we consider the
443 interactions described herein as the strongest evidence to date exemplifying chromatin
444 remodeler antagonism.

445 Evidence for RSC-Isw1 antagonism was revealed through two entirely independent,
446 unbiased genetic screens for suppression of RSC mutants. The first screen utilized an
447 SGA method to identify suppressors of *rsc7*Δ, and revealed *isw1*Δ as the strongest of four
448 identified gene suppressors, and the only gene with a chromatin-related function. Indeed,
449 combinations of *rsc* mutants with mutations in chromatin factors are almost invariably
450 lethal (*rsc4*-HDAC combinations are a rare exception (Kasten et al. 2004)). The second
451 screen – involving *rsc2* suppression by histone mutations – yielded a small set of mild
452 suppressors in histone H3 and one suppressor of moderate strength, H4 RH17,18CY.
453 This region of the H4 tail is known as the 'basic patch' – an epitope of known importance
454 for the binding and activity of several chromatin-modifying factors including ISWI, Sir3,
455 and Dot1 (Clapier et al. 2001; Clapier, Nightingale, and Becker 2002; Altaf et al. 2007;
456 Fingerman, Li, and Briggs 2007). Further genetic work focused the impact of this
457 mutation on ISWI function, then on Isw1 function, and finally on Isw1a function (as
458 opposed to the compositionally distinct Isw1b complex). Notably, combinations of *isw1*Δ
459 with Swi/Snf mutations did not confer suppression, indicating specificity for suppressing
460 RSC function. Taken together, two independent genetic screens, combined with multiple
461 additional genetic approaches, identify a specific suppression relationship between the
462 RSC complex and the Isw1a complex.

463 This RSC-ISW1a suppression is also consistent with a recent report that loss of Isw1a
464 complex can suppress the phenotypes of *gcn5*Δ mutations combined with loss of another

H3 acetyltransferase, Sas3 (Lafon, Petty, and Pillus 2012). It is possible that the *isw1*Δ and *ioc3*Δ suppression of *gcn5*Δ *sas3*Δ may be partially due to reducing the phenotypic effects of reduced acetylation by reducing RSC activity, since RSC function is partially dependent on acetylation (VanDemark et al. 2007).

We then explored whether this suppression relationship resulted from opposing roles of the two remodelers for regulating chromatin structure. A role for RSC at maintaining proper chromatin structure was previously demonstrated through the use of the strong *Sth1* degron allele (Parnell, Huff, and Cairns 2008; Hartley and Madhani 2009) and other RSC alleles (Badis et al. 2008; Ganguli et al. 2014). Loss of RSC function results in a gain of nucleosome density across Pol III genes and at the NDR of many Pol II genes. A clear observation here is the 'leftward' shift of the +1 and subsequent nucleosomes towards the NDR. This is consistent with (and extends) published models that RSC maintains the NDR by moving and/or ejecting nucleosomes from the TSS. Our work suggests that this movement and "fill in" is, at least in part, performed by the ISWI family of remodelers, as we have demonstrated a reduction of the "fill in" in the *rsc isw1* double mutant. Cells lacking *ISW1* alone exhibit modest changes in the coding region (Tirosh, Sigal, and Barkai 2010; Ni et al. 2010; Yen et al. 2012), which may, in part, be due to the loss of the ISW1b complex, which is thought to act primarily in the coding region, as opposed to the ISW1a complex that acts at promoters (Morillon et al. 2003). Our work here provides the first molecular examination of *rsc isw1* double mutants (prompted by our genetic suppression relationships) demonstrating antagonism between these remodelers regarding the depth of the NDR, the occupancy and positioning of the +1 nucleosome, and the phasing of proximal nucleosomes in the coding region (Figure 7).

The clustering of gene promoters into different classes based on their chromatin response to the loss of RSC function also revealed an interesting insight regarding the organization of promoter chromatin (Figure 7). More responsive genes have an open/structured promoter, with a classic -1, NDR, and +1 nucleosome at uniform positions with respect to the TSS. These patterns are evolutionarily conserved and partially imposed by sequence (Ioshikhes et al. 2006; Tsankov et al. 2011), where the open promoters demonstrate a

higher enrichment of nucleosome exclusion sequences, such as tracts of AAAAA, and illustrated by the strong NDR in the prediction model. While sequence alone cannot entirely dictate chromatin structure (Zhang et al. 2009), chromatin remodelers like RSC are able to reinforce the NDR by moving nucleosomes out of the NDR. The increased likelihood of Rsc3 or Reb1 binding sites occurring within the NDR may help recruit RSC or other factors to promoters that require nucleosome sliding or ejection activity to maintain this open architecture (Badis et al. 2008; Hartley and Madhani 2009). However, we note that the transcriptional output from these open promoters appears less affected following RSC loss than at closed/structured promoters (see below).

In contrast, the genes that lack a uniform chromatin response to RSC loss tend to have a closed or covered promoter, where nucleosomes are not uniformly positioned with respect to the TSS (Figure 7). This is not to say that these promoters have no chromatin structure at all; rather, each promoter has a unique chromatin structure that is not uniformly identical in phasing. In composite measurements, such as those presented in Figure 5B, these promoters appear to have little chromatin structure, when, in reality, they simply lack consensus structure. These promoters have an increased likelihood to have a TATA box and other transcription factor binding sites, whose access may be regulated by the partial occlusion by nucleosomes (Ioshikhes et al. 2006; Tirosh and Barkai 2008). Here, Isw1a may function to help assemble/mature and properly space nucleosomes at these promoters to repress transcription, which then increases their reliance upon remodelers such as RSC and/or SWI/SNF to expose these binding sites for proper activation. Hence, these promoters would have an increased presence of both activating and repressing chromatin remodelers, as well as histone turnover; both of which we observe (Figure 7). This continual state of flux, as well as lack of uniformity, may help explain why we observe little collective change in the chromatin structure in the absence of RSC function, while also observing a greater reliance on RSC function to maintain an active transcriptional status.

Taken together, our study provides the first evidence for an antagonistic relationship between RSC and ISWI, showing the genetic suppression of growth phenotypes and the lessening of chromatin impact due to the loss of RSC function. These effects are revealed

525 on a genome-wide scale, and further reveals that particular promoter chromatin
526 architectures can influence the degree of impact. These results reveal the different
527 strategies chromatin employed by genes for maintaining and regulating genic
528 transcription through the use of promoter architecture, DNA accessibility, and the
529 antagonism between complexes that act on promoter chromatin.

530

Materials and Methods

Media, Genetic Methods, and Strains

Rich media (YPD), synthetic complete (SC), minimal synthetic defined (SD), and sporulation media were prepared by standard methods. Standard procedures were used for transformations, sporulation, and tetrad analysis. All strains are derivatives of S288C, and full strain genotypes are listed in Supplemental File 1. Plasmids used are listed in Supplemental File 2. Null mutations in *ISW1* or *IOC3* were obtained from Invitrogen and crossed in, or made by PCR disruption, and confirmed by PCR and complementation.

Genetic screens for suppressors of *rsc2* and *rsc7* temperature sensitive mutants

To isolate mutations in Histone H3 or Histone H4 which could suppress a *rsc2* TS^- mutant, p1411 [*HHT2-HHF2.TRP1*] was mutagenized with hydroxylamine and transformed into YBC2140 (*rsc1*Δ *rsc2-V457M hht1*Δ-*hhf1*Δ *hht2*Δ*hhf2*Δ [*HHT2-HHF2.URA3*]). Approximately 20,000 transformants were plated to SC-TRP + 5FOA medium, incubated at 33˚C, and screened for colony growth. Resident plasmids conferring suppression were isolated, retransformed and sequenced.

The synthetic genetic array (SGA) screen was performed by mating *rsc7*Δ [*RSC7.URA3*] (YBC2039) with the yeast haploid deletion set (BY4741) from Invitrogen, and isolating double mutants as described in (Wilson et al. 2006). Double mutants were scored for the ability to grow at 35°C following *RSC7* plasmid loss on 5FOA.

RSC and ISW1 ChIP analysis

RSC8, *SNF2,* and *IOC3* genes were tagged endogenously with 13xMyc tags as described (Longtine et al. 1998). Yeast strains were grown in either rich media (YPD) or minimal media (SD), and ChIP performed from both samples as described previously (Parnell, Huff, and Cairns 2008). ChIP eluates and input DNA were labeled with either Cy5 or Cy3, and two biological replicates of each were hybridized to Agilent 244K microarrays.

552 The ChIP efficiency was better in cells grown in SD media, perhaps due to increased
553 cross-linking efficiency (rich media may inherently have a quenching effect relative to
554 minimal media). Comparison between YPD and SD derived occupancies revealed little
555 differences besides the relative scale of enrichment; therefore, all analysis was performed
556 using the SD data.

557 For ChIP sequencing the Rsc8-Myc, Ioc3-Myc, and Snf2-Myc strains were used in
558 addition to a strain expressing Sth1 tagged with 2xFlag under a Met25 promoter. ChIP
559 conditions were similar to those used previously except chromatin was liberated by
560 micrococcal nuclease. Immunoprecipitated products and corresponding input were
561 assembled into a library using Illumina protocols. Library products were size-selected for
562 mono-nucleosomes prior to paired-end sequencing (36 bp for Rsc8, 50 bp for remainder)
563 using Illumina sequencers.

HybMap RNA preparation

564 The HybMap microarray was custom designed to represent genes with a range of RSC
565 and ISW1 occupancies, and included 448 coding genes, 93 tRNA genes, and 52 non-
566 coding genes. Gene regions were extended by either 300 bp (coding and non-coding) or
567 150 bp (tRNA). Probes were selected from a pool of tiled 60mers and adjusted for length
568 to match melting temperatures as necessary. Both strands for each probe were included in
569 the design. Probes have a mean spacing of ~50 bp. As a control, 502 probes with
570 sequences from zebrafish were included as non-hybridizing control probes; sequences
571 were confirmed not to have significant homology to yeast sequences. Microarray designs
572 were submitted to Agilent Technologies for production as 4x44K arrays. Total RNA from
573 three biological replicates was prepared from each yeast strain, hybridized to the array,
574 and detected as described (Dutrow et al. 2008).

Nucleosome preparation

575 Yeast strains were grown under degron-inducing conditions and mono-nucleosomal DNA
576 was isolated as described previously (Parnell, Huff, and Cairns 2008). DNA fragments
577 were size-selected by agarose gel electrophoresis, purified, and labeled with either Cy3 or

Cy5. Labeled DNA from three biological replicates was co-hybridized to Agilent 244K microarrays for each strain. For sequencing, mono-nucleosomal DNA was prepared into a library using Illumina kits and subjected to paired-end 50 bp sequencing.

Bioinformatic analysis

Raw microarray data were quantile normalized, averaged, median-scaled, and assigned to genomic coordinates. For the HybMap protocol, probe values were median-scaled to the median intensity from the zebrafish control probes. Probe sequences were mapped to the *S. cerevisiae* genome version 64 (Saccharomyces Genome Database). Gene transcript models were based on whole-genome transcriptome data (Xu et al. 2009). Transcription start and stop sites were generated from processed transcriptome data, and compared and merged with published transcript models. Transcripts with discrepancies were manually curated using published occupancy maps for nucleosome and promoter initiation factors as guides. This resulted in a list of 5,338 high quality transcript models. For ChIP sequencing data, including published datasets obtained through NCBI, raw Fastq alignments were aligned using Novoalign and processed using the MACS2 software (https://github.com/taoliu/MACS) to generate fold enrichment data.

Most analysis was performed using BioToolBox (https://github.com/tjparnell/biotoolbox). Cluster analysis was visualized with Java Treeview (Saldanha 2004). Statistics and graphs were generated with Graphpad Prism (GraphPad Software, Inc.). Intersection analysis was performed with the USeq package (Nix, Courdy, and Boucher 2008). ChIP enrichment FDR values were calculated using MACS2.

Supplemental information

Supplemental Figures and Files are available. Raw microarray and sequencing data is available at GEO under accession number GSE65594.

Acknowledgements

We thank Sharon Dent, Toshio Tsukiyama, and Kevin Struhl for strains and/or plasmids. We thank HHMI and NIH (GM60415) for funding. We thank Melinda Angus-Hill for insight into *isw1*Δ suppression of *rsc3-3*; Shan-Fu Wu for assistance in strain generation; and members of the Cairns lab, Mahesh Chandrasekharan, and Tim Formosa for discussion.

References

Albert, I., T. N. Mavrich, L. P. Tomsho, J. Qi, S. J. Zanton, S. C. Schuster, and B. F. Pugh. 2007. "Translational and rotational settings of H2A.Z nucleosomes across the Saccharomyces cerevisiae genome." *Nature* no. 446 (7135):572-6. doi: 10.1038/nature05632.

Altaf, M., R. T. Utley, N. Lacoste, S. Tan, S. D. Briggs, and J. Cote. 2007. "Interplay of chromatin modifiers on a short basic patch of histone H4 tail defines the boundary of telomeric heterochromatin." *Mol Cell* no. 28 (6):1002-14. doi: 10.1016/j.molcel.2007.12.002.

Angus-Hill, M. L., A. Schlichter, D. Roberts, H. Erdjument-Bromage, P. Tempst, and B. R. Cairns. 2001. "A Rsc3/Rsc30 zinc cluster dimer reveals novel roles for the chromatin remodeler RSC in gene expression and cell cycle control." *Mol Cell* no. 7 (4):741-51. doi: 10.1016/S1097-2765(01)00219-2.

Badis, G., E. T. Chan, H. van Bakel, L. Pena-Castillo, D. Tillo, K. Tsui, C. D. Carlson, A. J. Gossett, M. J. Hasinoff, C. L. Warren, M. Gebbia, S. Talukder, A. Yang, S. Mnaimneh, D. Terterov, D. Coburn, A. Li Yeo, Z. X. Yeo, N. D. Clarke, J. D. Lieb, A. Z. Ansari, C. Nislow, and T. R. Hughes. 2008. "A library of yeast transcription factor motifs reveals a widespread function for Rsc3 in targeting nucleosome exclusion at promoters." *Mol Cell* no. 32 (6):878-87. doi: 10.1016/j.molcel.2008.11.020.

Bartholomew, B. 2014. "Regulating the chromatin landscape: structural and mechanistic perspectives." *Annu Rev Biochem* no. 83:671-96. doi: 10.1146/annurev-biochem-051810-093157.

Boeger, H., J. Griesenbeck, J. S. Strattan, and R. D. Kornberg. 2004. "Removal of promoter nucleosomes by disassembly rather than sliding in vivo." *Mol Cell* no. 14 (5):667-73. doi: 10.1016/j.molcel.2004.05.013.

Cairns, B. R. 2009. "The logic of chromatin architecture and remodelling at promoters." *Nature* no. 461 (7261):193-8. doi: 10.1038/nature08450.

Cairns, B. R., Y. Lorch, Y. Li, M. Zhang, L. Lacomis, H. Erdjument-Bromage, P. Tempst, J. Du, B. Laurent, and R. D. Kornberg. 1996. "RSC, an essential, abundant chromatin-remodeling complex." *Cell* no. 87 (7):1249-60.

Cairns, B. R., A. Schlichter, H. Erdjument-Bromage, P. Tempst, R. D. Kornberg, and F. Winston. 1999. "Two functionally distinct forms of the RSC nucleosome-remodeling complex, containing essential AT hook, BAH, and bromodomains." *Mol Cell* no. 4 (5):715-23.

Carey, M., B. Li, and J. L. Workman. 2006. "RSC exploits histone acetylation to abrogate the nucleosomal block to RNA polymerase II elongation." *Mol Cell* no. 24 (3):481-7. doi: 10.1016/j.molcel.2006.09.012.

Clapier, C. R., and B. R. Cairns. 2009. "The biology of chromatin remodeling complexes." *Annu Rev Biochem* no. 78:273-304. doi: 10.1146/annurev.biochem.77.062706.153223.

Clapier, C. R., G. Langst, D. F. Corona, P. B. Becker, and K. P. Nightingale. 2001. "Critical role for the histone H4 N terminus in nucleosome remodeling by ISWI." *Mol Cell Biol* no. 21 (3):875-83. doi: 10.1128/MCB.21.3.875-883.2001.

Clapier, C. R., K. P. Nightingale, and P. B. Becker. 2002. "A critical epitope for substrate recognition by the nucleosome remodeling ATPase ISWI." *Nucleic Acids Res* no. 30 (3):649-55.

Dechassa, M. L., A. Sabri, S. Pondugula, S. R. Kassabov, N. Chatterjee, M. P. Kladde, and B. Bartholomew. 2010. "SWI/SNF has intrinsic nucleosome disassembly activity that is dependent on adjacent nucleosomes." *Mol Cell* no. 38 (4):590-602. doi: 10.1016/j.molcel.2010.02.040.

Dutrow, N., D. A. Nix, D. Holt, B. Milash, B. Dalley, E. Westbroek, T. J. Parnell, and B. R. Cairns. 2008. "Dynamic transcriptome of Schizosaccharomyces pombe shown by RNA-DNA hybrid mapping." *Nat Genet* no. 40 (8):977-86. doi: 10.1038/ng.196.

Fazzio, T. G., M. E. Gelbart, and T. Tsukiyama. 2005. "Two distinct mechanisms of chromatin interaction by the Isw2 chromatin remodeling complex in vivo." *Mol Cell Biol* no. 25 (21):9165-74. doi: 10.1128/MCB.25.21.9165-9174.2005.

Fazzio, T. G., C. Kooperberg, J. P. Goldmark, C. Neal, R. Basom, J. Delrow, and T. Tsukiyama. 2001. "Widespread collaboration of Isw2 and Sin3-Rpd3 chromatin remodeling complexes in transcriptional repression." *Mol Cell Biol* no. 21 (19):6450-60.

Ferreira, H., A. Flaus, and T. Owen-Hughes. 2007. "Histone modifications influence the action of Snf2 family remodelling enzymes by different mechanisms." *J Mol Biol* no. 374 (3):563-79. doi: 10.1016/j.jmb.2007.09.059.

Fingerman, I. M., H. C. Li, and S. D. Briggs. 2007. "A charge-based interaction between histone H4 and Dot1 is required for H3K79 methylation and telomere silencing: identification of a new trans-histone pathway." *Genes Dev* no. 21 (16):2018-29. doi: 10.1101/gad.1560607.

Flowers, S., N. G. Nagl, Jr., G. R. Beck, Jr., and E. Moran. 2009. "Antagonistic roles for BRM and BRG1 SWI/SNF complexes in differentiation." *J Biol Chem* no. 284 (15):10067-75. doi: 10.1074/jbc.M808782200.

Gangaraju, V. K., and B. Bartholomew. 2007. "Dependency of ISW1a chromatin remodeling on extranucleosomal DNA." *Mol Cell Biol* no. 27 (8):3217-25. doi: 10.1128/MCB.01731-06.

Ganguli, D., R. V. Chereji, J. R. Iben, H. A. Cole, and D. J. Clark. 2014. "RSC-dependent constructive and destructive interference between opposing arrays of phased nucleosomes in yeast." *Genome Res* no. 24 (10):1637-49. doi: 10.1101/gr.177014.114.

Grune, T., J. Brzeski, A. Eberharter, C. R. Clapier, D. F. Corona, P. B. Becker, and C. W. Muller. 2003. "Crystal structure and functional analysis of a

nucleosome recognition module of the remodeling factor ISWI." *Mol Cell* no. 12 (2):449-60.

Hartley, P. D., and H. D. Madhani. 2009. "Mechanisms that specify promoter nucleosome location and identity." *Cell* no. 137 (3):445-58. doi: 10.1016/j.cell.2009.02.043.

Howe, L., D. Auston, P. Grant, S. John, R. G. Cook, J. L. Workman, and L. Pillus. 2001. "Histone H3 specific acetyltransferases are essential for cell cycle progression." *Genes Dev* no. 15 (23):3144-54. doi: 10.1101/gad.931401.

Ioshikhes, I. P., I. Albert, S. J. Zanton, and B. F. Pugh. 2006. "Nucleosome positions predicted through comparative genomics." *Nat Genet* no. 38 (10):1210-5. doi: 10.1038/ng1878.

Johnsson, A., M. Durand-Dubief, Y. Xue-Franzen, M. Ronnerblad, K. Ekwall, and A. Wright. 2009. "HAT-HDAC interplay modulates global histone H3K14 acetylation in gene-coding regions during stress." *EMBO Rep* no. 10 (9):1009-14. doi: 10.1038/embor.2009.127.

Josling, G. A., S. A. Selvarajah, M. Petter, and M. F. Duffy. 2012. "The role of bromodomain proteins in regulating gene expression." *Genes (Basel)* no. 3 (2):320-43. doi: 10.3390/genes3020320.

Kaplan, N., I. K. Moore, Y. Fondufe-Mittendorf, A. J. Gossett, D. Tillo, Y. Field, E. M. LeProust, T. R. Hughes, J. D. Lieb, J. Widom, and E. Segal. 2009. "The DNA-encoded nucleosome organization of a eukaryotic genome." *Nature* no. 458 (7236):362-6. doi: 10.1038/nature07667.

Kasten, M., H. Szerlong, H. Erdjument-Bromage, P. Tempst, M. Werner, and B. R. Cairns. 2004. "Tandem bromodomains in the chromatin remodeler RSC recognize acetylated histone H3 Lys14." *Embo j* no. 23 (6):1348-59. doi: 10.1038/sj.emboj.7600143.

Lafon, A., E. Petty, and L. Pillus. 2012. "Functional antagonism between Sas3 and Gcn5 acetyltransferases and ISWI chromatin remodelers." *PLoS Genet* no. 8 (10):e1002994. doi: 10.1371/journal.pgen.1002994.

Lee, W., D. Tillo, N. Bray, R. H. Morse, R. W. Davis, T. R. Hughes, and C. Nislow. 2007. "A high-resolution atlas of nucleosome occupancy in yeast." *Nat Genet* no. 39 (10):1235-44. doi: 10.1038/ng2117.

Longtine, M. S., A. McKenzie, 3rd, D. J. Demarini, N. G. Shah, A. Wach, A. Brachat, P. Philippsen, and J. R. Pringle. 1998. "Additional modules for versatile and economical PCR-based gene deletion and modification in Saccharomyces cerevisiae." *Yeast* no. 14 (10):953-61. doi: 10.1002/(SICI)1097-0061(199807)14:10<953::AID-YEA293>3.0.CO;2-U.

Lorch, Y., M. Zhang, and R. D. Kornberg. 1999. "Histone octamer transfer by a chromatin-remodeling complex." *Cell* no. 96 (3):389-92.

Millar, C. B., S. K. Kurdistani, and M. Grunstein. 2004. "Acetylation of yeast histone H4 lysine 16: a switch for protein interactions in heterochromatin and euchromatin." *Cold Spring Harb Symp Quant Biol* no. 69:193-200. doi: 10.1101/sqb.2004.69.193.

Morillon, A., N. Karabetsou, J. O'Sullivan, N. Kent, N. Proudfoot, and J. Mellor. 2003. "Isw1 chromatin remodeling ATPase coordinates transcription elongation and termination by RNA polymerase II." *Cell* no. 115 (4):425-35.

Musladin, S., N. Krietenstein, P. Korber, and S. Barbaric. 2014. "The RSC chromatin remodeling complex has a crucial role in the complete remodeler set for yeast PHO5 promoter opening." *Nucleic Acids Res* no. 42 (7):4270-82. doi: 10.1093/nar/gkt1395.

Nagalakshmi, U., Z. Wang, K. Waern, C. Shou, D. Raha, M. Gerstein, and M. Snyder. 2008. "The transcriptional landscape of the yeast genome defined by RNA sequencing." *Science* no. 320 (5881):1344-9. doi: 10.1126/science.1158441.

Narlikar, G. J., R. Sundaramoorthy, and T. Owen-Hughes. 2013. "Mechanisms and functions of ATP-dependent chromatin-remodeling enzymes." *Cell* no. 154 (3):490-503. doi: 10.1016/j.cell.2013.07.011.

Ng, H. H., F. Robert, R. A. Young, and K. Struhl. 2002. "Genome-wide location and regulated recruitment of the RSC nucleosome-remodeling complex." *Genes Dev* no. 16 (7):806-19. doi: 10.1101/gad.978902.

Ni, T., K. Tu, Z. Wang, S. Song, H. Wu, B. Xie, K. C. Scott, S. I. Grewal, Y. Gao, and J. Zhu. 2010. "The prevalence and regulation of antisense transcripts in Schizosaccharomyces pombe." *PLoS One* no. 5 (12):e15271. doi: 10.1371/journal.pone.0015271.

Nix, D. A., S. J. Courdy, and K. M. Boucher. 2008. "Empirical methods for controlling false positives and estimating confidence in ChIP-Seq peaks." *BMC Bioinformatics* no. 9:523. doi: 10.1186/1471-2105-9-523.

Parkhomchuk, D., T. Borodina, V. Amstislavskiy, M. Banaru, L. Hallen, S. Krobitsch, H. Lehrach, and A. Soldatov. 2009. "Transcriptome analysis by strand-specific sequencing of complementary DNA." *Nucleic Acids Res* no. 37 (18):e123. doi: 10.1093/nar/gkp596.

Parnell, T. J., J. T. Huff, and B. R. Cairns. 2008. "RSC regulates nucleosome positioning at Pol II genes and density at Pol III genes." *Embo j* no. 27 (1):100-10. doi: 10.1038/sj.emboj.7601946.

Ramirez-Carrozzi, V. R., A. A. Nazarian, C. C. Li, S. L. Gore, R. Sridharan, A. N. Imbalzano, and S. T. Smale. 2006. "Selective and antagonistic functions of SWI/SNF and Mi-2beta nucleosome remodeling complexes during an inflammatory response." *Genes Dev* no. 20 (3):282-96. doi: 10.1101/gad.1383206.

Raser, J. M., and E. K. O'Shea. 2004. "Control of stochasticity in eukaryotic gene expression." *Science* no. 304 (5678):1811-4. doi: 10.1126/science.1098641.

Rufiange, A., P. E. Jacques, W. Bhat, F. Robert, and A. Nourani. 2007. "Genome-wide replication-independent histone H3 exchange occurs predominantly at promoters and implicates H3 K56 acetylation and Asf1." *Mol Cell* no. 27 (3):393-405. doi: 10.1016/j.molcel.2007.07.011.

Saha, A., J. Wittmeyer, and B. R. Cairns. 2002. "Chromatin remodeling by RSC involves ATP-dependent DNA translocation." *Genes Dev* no. 16 (16):2120-34. doi: 10.1101/gad.995002.

———. 2005. "Chromatin remodeling through directional DNA translocation from an internal nucleosomal site." *Nat Struct Mol Biol* no. 12 (9):747-55. doi: 10.1038/nsmb973.

Saldanha, A. J. 2004. "Java Treeview--extensible visualization of microarray data." *Bioinformatics* no. 20 (17):3246-8. doi: 10.1093/bioinformatics/bth349.

Santos-Rosa, H., R. Schneider, B. E. Bernstein, N. Karabetsou, A. Morillon, C. Weise, S. L. Schreiber, J. Mellor, and T. Kouzarides. 2003. "Methylation of histone H3 K4 mediates association of the Isw1p ATPase with chromatin." *Mol Cell* no. 12 (5):1325-32.

Schlichter, A., and B. R. Cairns. 2005. "Histone trimethylation by Set1 is coordinated by the RRM, autoinhibitory, and catalytic domains." *Embo j* no. 24 (6):1222-31. doi: 10.1038/sj.emboj.7600607.

Segal, E., Y. Fondufe-Mittendorf, L. Chen, A. Thastrom, Y. Field, I. K. Moore, J. P. Wang, and J. Widom. 2006. "A genomic code for nucleosome positioning." *Nature* no. 442 (7104):772-8. doi: 10.1038/nature04979.

Segal, E., and J. Widom. 2009. "Poly(dA:dT) tracts: major determinants of nucleosome organization." *Curr Opin Struct Biol* no. 19 (1):65-71. doi: 10.1016/j.sbi.2009.01.004.

Tirosh, I., and N. Barkai. 2008. "Two strategies for gene regulation by promoter nucleosomes." *Genome Res* no. 18 (7):1084-91. doi: 10.1101/gr.076059.108.

Tirosh, I., N. Sigal, and N. Barkai. 2010. "Widespread remodeling of mid-coding sequence nucleosomes by Isw1." *Genome Biol* no. 11 (5):R49. doi: 10.1186/gb-2010-11-5-r49.

Tomar, R. S., J. N. Psathas, H. Zhang, Z. Zhang, and J. C. Reese. 2009. "A novel mechanism of antagonism between ATP-dependent chromatin remodeling complexes regulates RNR3 expression." *Mol Cell Biol* no. 29 (12):3255-65. doi: 10.1128/MCB.01741-08.

Tong, A. H., M. Evangelista, A. B. Parsons, H. Xu, G. D. Bader, N. Page, M. Robinson, S. Raghibizadeh, C. W. Hogue, H. Bussey, B. Andrews, M. Tyers, and C. Boone. 2001. "Systematic genetic analysis with ordered arrays of yeast deletion mutants." *Science* no. 294 (5550):2364-8. doi: 10.1126/science.1065810.

Tsankov, A., Y. Yanagisawa, N. Rhind, A. Regev, and O. J. Rando. 2011. "Evolutionary divergence of intrinsic and trans-regulated nucleosome

positioning sequences reveals plastic rules for chromatin organization." *Genome Res* no. 21 (11):1851-62. doi: 10.1101/gr.122267.111.

Tsukiyama, T., J. Palmer, C. C. Landel, J. Shiloach, and C. Wu. 1999. "Characterization of the imitation switch subfamily of ATP-dependent chromatin-remodeling factors in Saccharomyces cerevisiae." *Genes Dev* no. 13 (6):686-97.

van Bakel, H., K. Tsui, M. Gebbia, S. Mnaimneh, T. R. Hughes, and C. Nislow. 2013. "A compendium of nucleosome and transcript profiles reveals determinants of chromatin architecture and transcription." *PLoS Genet* no. 9 (5):e1003479. doi: 10.1371/journal.pgen.1003479.

VanDemark, A. P., M. M. Kasten, E. Ferris, A. Heroux, C. P. Hill, and B. R. Cairns. 2007. "Autoregulation of the rsc4 tandem bromodomain by gcn5 acetylation." *Mol Cell* no. 27 (5):817-28. doi: 10.1016/j.molcel.2007.08.018.

Vary, J. C., Jr., V. K. Gangaraju, J. Qin, C. C. Landel, C. Kooperberg, B. Bartholomew, and T. Tsukiyama. 2003. "Yeast Isw1p forms two separable complexes in vivo." *Mol Cell Biol* no. 23 (1):80-91.

Vignali, M., A. H. Hassan, K. E. Neely, and J. L. Workman. 2000. "ATP-dependent chromatin-remodeling complexes." *Mol Cell Biol* no. 20 (6):1899-910.

Wang, F., G. Li, M. Altaf, C. Lu, M. A. Currie, A. Johnson, and D. Moazed. 2013. "Heterochromatin protein Sir3 induces contacts between the amino terminus of histone H4 and nucleosomal DNA." *Proc Natl Acad Sci U S A* no. 110 (21):8495-500. doi: 10.1073/pnas.1300126110.

Whitehouse, I., A. Flaus, B. R. Cairns, M. F. White, J. L. Workman, and T. Owen-Hughes. 1999. "Nucleosome mobilization catalysed by the yeast SWI/SNF complex." *Nature* no. 400 (6746):784-7. doi: 10.1038/23506.

Whitehouse, I., O. J. Rando, J. Delrow, and T. Tsukiyama. 2007. "Chromatin remodelling at promoters suppresses antisense transcription." *Nature* no. 450 (7172):1031-5. doi: 10.1038/nature06391.

Whitehouse, I., and T. Tsukiyama. 2006. "Antagonistic forces that position nucleosomes in vivo." *Nat Struct Mol Biol* no. 13 (7):633-40. doi: 10.1038/nsmb1111.

Wilson, B., H. Erdjument-Bromage, P. Tempst, and B. R. Cairns. 2006. "The RSC chromatin remodeling complex bears an essential fungal-specific protein module with broad functional roles." *Genetics* no. 172 (2):795-809. doi: 10.1534/genetics.105.047589.

Xu, Z., W. Wei, J. Gagneur, F. Perocchi, S. Clauder-Munster, J. Camblong, E. Guffanti, F. Stutz, W. Huber, and L. M. Steinmetz. 2009. "Bidirectional promoters generate pervasive transcription in yeast." *Nature* no. 457 (7232):1033-7. doi: 10.1038/nature07728.

Yamada, K., T. D. Frouws, B. Angst, D. J. Fitzgerald, C. DeLuca, K. Schimmele, D. F. Sargent, and T. J. Richmond. 2011. "Structure and mechanism of the chromatin remodelling factor ISW1a." *Nature* no. 472 (7344):448-53. doi: 10.1038/nature09947.

Yen, K., V. Vinayachandran, K. Batta, R. T. Koerber, and B. F. Pugh. 2012. "Genome-wide nucleosome specificity and directionality of chromatin remodelers." *Cell* no. 149 (7):1461-73. doi: 10.1016/j.cell.2012.04.036.

Yuan, G. C., Y. J. Liu, M. F. Dion, M. D. Slack, L. F. Wu, S. J. Altschuler, and O. J. Rando. 2005. "Genome-scale identification of nucleosome positions in S. cerevisiae." *Science* no. 309 (5734):626-30. doi: 10.1126/science.1112178.

Zentner, G. E., and S. Henikoff. 2013. "Regulation of nucleosome dynamics by histone modifications." *Nat Struct Mol Biol* no. 20 (3):259-66. doi: 10.1038/nsmb.2470.

Zhang, Y., Z. Moqtaderi, B. P. Rattner, G. Euskirchen, M. Snyder, J. T. Kadonaga, X. S. Liu, and K. Struhl. 2009. "Intrinsic histone-DNA interactions are not the major determinant of nucleosome positions in vivo." *Nat Struct Mol Biol* no. 16 (8):847-52. doi: 10.1038/nsmb.1636.

Figure Titles and Legends

Figure 1. Suppressors of *rsc2* and *rsc7* alleles obtained by genetic screen

(A) Suppression of the *rsc7*Δ temperature sensitivity by the *isw1*Δ mutation. Wild-type (YBC62) and *rsc7*Δ (YBC2039) were transformed with plasmids containing *RSC7*, *ISW1* or empty vector, and spotted as five-fold serial dilutions to SC-URA media, and grown at 35°. (B) Histone H3 and H4 suppressors of *rsc2-V457M.* YBC2140 (*rsc1*Δ *rsc2-V457M hht1-hhf1 hht2-hhf2* [*H3-H4.URA*]*)* was transformed with *TRP1* marked plasmids bearing histone mutations, streaked to SC-TRP + 5FOA to force loss of the WT histone plasmid, and then spotted as tenfold serial dilutions to SC-TRP at 30°C or 33°C. (C) Tenfold dilutions of YBC2140 transformed with H3 or H4 mutations, and spotted to SC-TRP + 5FOA at 30°C or 33°C. Figure Supplement 1 shows that Rsc2 alleles are not suppressed by *dot1*Δ or *sir3*Δ.

Figure 2. A null mutation of *isw1* suppresses RSC mutations.

(A) rsc2 Ts^- alleles are suppressed by *isw1*Δ. An *ISW1*+ strain (YBC1231; *rsc1*Δ *rsc2*Δ [*RSC1.URA3*]) and an *isw1*Δ strain (YBC1479; *rsc1*Δ *rsc2*Δ *isw1*Δ [*RSC1.URA*]), were transformed with *TRP1* marked RSC2 (p604), *rsc2-V457M* (p776), or *rsc2*$^-$*D461G* (p777), streaked to SC-TRP + 5FOA to force loss of the RSC1 plasmid, and then spotted as tenfold dilutions to YPD at 30°C, 33°C and YPD containing 1.5% Formamide (Form) or 12μg/ml Benomyl. (B) *isw1*Δ suppresses 6-azauracil (6AU) and mycophenolic acid (MPA) phenotypes of *rsc2* mutations. YBC1231 (*ISW1*+) and YBC1479 (*isw1*Δ) were transformed with *TRP1* marked *RSC2* (p776), *rsc2*$^-$*V457M* (p776), or *rsc2*$^-$ (YBC777), streaked to SC-TRP + 5FOA to force loss of the RSC1 plasmid, and then transformed with *URA3* marked vector. Strains were then streaked to SC-URA medium containing 20 μg/ml MPA or 150 μg/ml 6AU. (C) *isw1*Δ suppresses additional RSC mutations but does not suppress *snf2.* WT (YBC62), *isw1*Δ (YBC1416), *rsc2-V457M* (YBC1111), *rsc2-V457M isw1*Δ (YBC2810), *rsc3-3* (YBC906), *rsc3-3 isw1*Δ (YBC1485 p817) *rsc4-2* (YBC1278), *rsc4-2 isw1*Δ (YBC2867), *rsc7*Δ (YBC1333), *rsc7*Δ *isw1*Δ (YBC2233),

*snf2*Δ (YBC26), and *snf2*Δ *isw1*Δ (YBC2812) were spotted as tenfold serial dilutions to YPD 30°C, 33°C, 35°C, 38°C, YPD containing 150mM Hydroxyurea (HU), and YPGal + Antimycin A (AA). Figure Supplement 1 shows suppression of *rsc2* alleles by catalytic *isw1* and *isw2*Δ mutants.

Figure 3. Suppression of *RSC* mutants is specific to Isw1a.

(A) *rsc2-V457M* is lethal in combination with *ioc2*Δ and *ioc4*Δ*,* but not *ioc3*Δ*.* YBC803 (*rsc1*Δ *rsc2*Δ [*RSC1.URA3*]), YBC2730 (*rsc1*Δ *rsc2*Δ *ioc3*Δ [*RSC1.URA3*]), YBC2729 (*rsc1*Δ *rsc2*Δ *ioc2*Δ [*RSC1.URA3*]), and YBC2731 (*rsc1*Δ *rsc2*Δ *ioc4*Δ [*RSC1.URA3*]), were transformed with *TRP1* marked *RSC2* (p604) or *rsc2-V457M* (p776), and spotted as tenfold dilutions to SC-TRP 30°C, or SC-TRP + 5FOA 30°C. (B) *rsc2* Ts^- mutations can be partially suppressed by *ioc3*Δ*.* YBC803 (*rsc1*Δ *rsc2*Δ [*RSC1.URA3*]), and YBC 2730 (*rsc1*Δ *rsc2*Δ *ioc3*Δ [*RSC1.URA3*]), were transformed with *TRP1* marked *RSC2* (p604), *rsc2-V457M* (p776) or *rsc2-D461G* (p777), streaked to SC-TRP + 5FOA to force loss of the *RSC1* plasmid, and then streaked to SC-TRP at 30°C or 32°C. (C) *rsc4-2* is suppressed by *ioc3*Δ*. rsc4* [*RSC4.URA3*]) and YBC3020 (*rsc4*Δ *ioc3*Δ [*RSC4.URA3*]) were transformed with *TRP1* marked *RSC4* (p1060) or *rsc4-2* (p1083), streaked to SC-TRP + 5FOA to lose *RSC4.URA3,* and then spotted as tenfold serial dilutions to SC-TRP 30°C or SC-TRP 38°C. Figure Supplement 1 shows suppression of *rsc1* mutants by *ioc3*Δ. Figure Supplement 2 shows the suppression of *rsc2* synthetic lethality with *set1*Δ and *gcn5*Δ by mutations in ISW1a.

Figure 4. RSC and ISW1a co-occupy many locations, and their loss impacts gene expression in a complex manner.

(A) Heat map of Rsc8 and Ioc3 protein occupancy as determined by ChIP at all transcription start sites (TSS). Each row represents a gene, with occupancy scored in 50 bp windows ±800 bp relative to the TSS (bent arrow). Windows overlapping neighboring genes are excluded. Occupancy above global mean is indicated in red, below in blue. Genes are clustered by a k-means algorithm into 6 groups. (B) The distributions of mean Rsc8 and Ioc3 occupancy values shown as box and whisker plots for different annotation

features. (C) The correlation between Rsc8 and Ioc3 at promoters shown as a XY plot, either genome-wide or restricted to the 500 coding genes selected for the custom HybMap microarray. (D) The distribution of the mean mutant/wildtype gene expression ratios as determined by the HybMap microarray for three classes of gene types are presented as box and whisker plots. Figure Supplement 1 compares the ChIP results obtained from microarray versus deep sequencing. Figure Supplement 2 displays the genes that appear suppressed by isw1Δ or ioc3Δ as determined by HybMap.

Figure 5. Loss of ISW1 partially suppresses nucleosomal changes exhibited by loss of RSC function.

(A) The promoter profile of nucleosome occupancy ratios between *sth1*^{td} degron (rscΔ) and control (RSC) strains is presented as a heat map, where red represents a gain in nucleosome occupancy and blue represents a loss. Genes (rows) are organized into six groups by k-means clustering. Columns represent 50 bp windows ±800 bp relative to the TSS. Windows overlapping neighboring genes are excluded. (B,C,D) The mean profiles of nucleosome occupancies for all genes within each cluster are shown. Profiles from mutant backgrounds are shown in red, and wild type profiles are shown in blue. The y-axis represents log2 occupancy relative to genome average. Figure Supplement compares the nucleosome profiles obtained from microarray and deep sequencing, as well as the predicted nucleosome occupancy.

Figure 6. Gene clusters identified by their response to RSC loss reveal different promoter classes.

(A) The relative expression in *rsc2* (left) or *isw1*Δ (right) mutants relative to wild type as measured by the HybMap assay are plotted as box and whisker distribution plots for each of the six gene clusters identified by their response to RSC loss. (B) The mean occupancy profile over each of the six gene clusters is presented for six different factors, including RSC, ISW1, SNF2, ISW2 (Zentner and Henikoff 2013), CHD1 (Zentner and Henikoff 2013), and H2AZ (Albert et al. 2007). (C) The mean profile for histone turnover over the six gene clusters is shown. Higher values represent higher turnover. (D) Heat map

representing the P-value significance for the intersection between genes in different categories. Open promoters include genes in clusters 1-4. Closed promoters include genes in clusters 5 and 6. Figure Supplement 1 shows the distribution of normal gene expression for each of the clusters. Figure Supplement 2 shows the occupancy profile for RSC and ISW1a as determined by deep sequencing.

Figure 7. Model of action by RSC and ISWI remodelers at open and closed promoters.

An open or structured promoter is depicted on the left with regularly spaced nucleosomes (yellow ovals) and a predominate NDR that frequently contains sequence elements (colored lines), including Rsc3 and Reb1 binding sites as well AT-rich sequence tracts unfavorable to nucleosome formation. Remodelers such as RSC (blue oval) help to maintain nucleosome deficiency, while ISWIa (orange oval) antagonizes by "filling in" the NDR. (Note: Rsc3 is not required for RSC activity, nor is Rsc3 required for all RSC recruitment.) In the absence of RSC, this filling in occurs and is conducted by ISW1a, as filling in is not observed in *rsc isw1* double mutants. A closed or unstructured promoter is depicted on the right, evidenced by the lack of a clearly defined NDR and obscured promoter sequence elements, such as the TATA. Nucleosome density (or likelihood of occupancy) is depicted by the opacity of the nucleosomes. These promoters have increased nucleosome movement and histone turnover (yellow arrows), likely aided by chromatin remodelers such as RSC and ISWI, which eject or reposition nucleosomes, respectively. In the absence of RSC, nucleosome ejection is reduced, leading to higher nucleosome density (opaque nucleosomes) and a reduction in transcription. Additional loss of ISW1a may reduce the assembly/organization of nucleosomes in the promoter, partially restoring transcription.

Figure 1 – Supplement 1. *Rsc2* mutations are not suppressed by *dot1*Δ or *sir3*Δ.

*(A) dot1*Δ does not suppress *rsc2-V457M.* YBC803 (*rsc1*Δ*rsc2*Δ [*RSC1.URA3*]) and YBC1683 (*rsc1*Δ *rsc2*Δ *dot1*Δ [*RSC1.URA3*]) were transformed with *TRP1* marked *RSC2* (p604) or *rsc2-V457M* (p776) and spotted to SC-TRP 30°C, and SC-TRP + 5FOA

30°C. (B) A null mutation in *SIR3* does not suppress *rsc2-V457M.* YBC803 (*rsc1*Δ*rsc2*Δ [*RSC1.URA3*]) and YBC3185 (*rsc1*Δ *rsc2*Δ *sir3*Δ [*RSC1.URA3*]) were transformed with *TRP1* marked *RSC2* (p604) or *rsc2-V457M* (p776) and spotted to SC-TRP 30°C, and SC-TRP + 5FOA 32°C.

Figure 2 – Supplement 1. *rsc2* mutations are suppressed by an *ISW1* ATPase mutation and an *ISW2* null mutation.

(A) Growth ability of *rsc2-V457M isw1*Δ at the nonpermissive temperature in the presence of *ISW1+,* or *ISW1-K227A.* (B) *rsc2* Ts^- alleles in combination with *isw2*Δ. An *ISW2+* strain (YBC1231; *rsc1*Δ *rsc2*Δ [*RSC1.URA3*]) and an *isw2*Δ strain (YBC1480; *rsc1*Δ *rsc2*Δ *isw2*Δ [*RSC1.URA3*]), were transformed with *TRP1* marked *RSC2* (p604), *rsc2- V457M* (p776), or *rsc2-D461G* (p777), streaked to SC-TRP + 5FOA to force loss of the RSC1 plasmid, and then spotted as tenfold dilutions to YPD at 30°C, 32°C and YPD containing 12µg/ml Benomyl. (C) *isw2*Δ suppresses 6-azauracil (6AU) and mycophenolic acid (MPA) phenotypes of *rsc2* mutations. YBC1231 (*ISW1+*) and YBC1480 (*isw2*Δ) were transformed with *TRP1* marked *RSC2* (p776), *rsc2 V457M* (p776), or *rsc2 D461G* (YBC777), streaked to SC-TRP + 5FOA to force loss of the RSC1 plasmid, and then transformed with *URA3* marked vector. Strains were then streaked to SC-URA medium containing 20 µg/ml MPA or 150 µg/ml 6-azauracil 6AU.

Figure 2 – Supplement 1. *rsc2* mutations are suppressed by an *ISW1* ATPase mutation and an *ISW2* null mutation.

(A) Growth ability of *rsc2-V457M isw1*Δ at the nonpermissive temperature in the presence of *ISW1+,* or *ISW1-K227A.* (B) *rsc2* Ts^- alleles in combination with *isw2*Δ. An *ISW2+* strain (YBC1231; *rsc1*Δ *rsc2*Δ [*RSC1.URA3*]) and an *isw2*Δ strain (YBC1480; *rsc1*Δ *rsc2*Δ *isw2*Δ [*RSC1.URA3*]), were transformed with *TRP1* marked *RSC2* (p604), *rsc2- V457M* (p776), or *rsc2-D461G* (p777), streaked to SC-TRP + 5FOA to force loss of the RSC1 plasmid, and then spotted as tenfold dilutions to YPD at 30°C, 32°C and YPD containing 12µg/ml Benomyl. (C) *isw2*Δ suppresses 6-azauracil (6AU) and mycophenolic acid (MPA) phenotypes of *rsc2* mutations. YBC1231 (*ISW1+*) and YBC1480 (*isw2*Δ)

were transformed with *TRP1* marked *RSC2* (p776), *rsc2 V457M* (p776), or *rsc2 D461G* (YBC777), streaked to SC-TRP + 5FOA to force loss of the RSC1 plasmid, and then transformed with *URA3* marked vector. Strains were then streaked to SC-URA medium containing 20 µg/ml MPA or 150 µg/ml 6-azauracil 6AU.

Figure 3 – Supplement 2. Synthetic lethality of *rsc2* mutations with *set1*Δ and *gcn5*Δ can be suppressed by *isw1* and *ioc3*.

(A) Mutations in *rsc2* that are synthetic lethal with loss of Set1 (the sole H3 K4 methyltransferase in yeast) are suppressed by null mutations in *ISW1* and *IOC3*. Strains with *rsc1*Δ *rsc2*Δ *set1*Δ [*RSC1.URA3*] (YBC1245) were combined with *isw1*Δ (YBC2744) or *ioc3*Δ (YBC2803), transformed with *TRP1* marked plasmids *RSC2* (p604), *rsc2-V457M* (p776), or *rsc2-D461G* (p777), and spotted as tenfold serial dilutions to SC-TRP and SC-TRP + 5FOA (to enforce loss of the *RSC1* plasmid) at 30°C. Additionally, we combined each of the *rsc2 isw1*Δ mutant combinations with hyperactive $Set1^{D}$ alleles (Schlichter and Cairns 2005), and did not see further suppression (data not shown). (B) Synthetic lethality of *rsc2*Δ with loss of the histone acetyltransferase Gcn5 is suppressed by *isw1*Δ. YBC3496 (*rsc2*Δ), YBC 3494 (*rsc2*Δ *gcn5*Δ), and YBC3495 (*rsc2*Δ *gcn5*Δ *isw1*Δ) each covered with [p199; *RSC2.URA3*] were spotted as tenfold serial dilutions to SC 30°C and SC + 5FOA 30°C.

Figure 4 – Supplement 1. RSC and ISW1a occupancy correlate between microarray and sequence studies.

Heat map of RSC (A) and ISW1a (B) occupancies. RSC occupancy was determined by Rsc8 ChIP applied to microarray (MA), Rsc8 ChIP paired-end sequencing (Seq), and Sth1 paired-end sequencing. ISW1a occupancy was determined by Ioc3 ChIP applied to microarray and Ioc3 ChIP paired-end sequencing. Occupancy, expressed as log2 fold enrichment over input, was measured in 20 bp windows flanking the TSS ±800 bp; windows overlapping neighboring genes were excluded. Genes were organized into six clusters using a k-means algorithm based on the Rsc8 microarray occupancy and is identical to Figure 4. Only windows with positive (enriched) values (red) are plotted to

simplify visualization. (C) To show correlation between the microarray and sequencing datasets, the maximum occupancy value for each gene determined in a 500 bp window encompassing the TSS (±250 bp) was plotted as a pairwise scatter plot, with the microarray dataset on the X axis for each plot. A linear regression line is plotted as a thick black line.

Figure 4 – Supplement 2. Some genes show transcriptional suppression in *rsc2 isw1*Δ double mutants.

The change in expression relative to wild type as determined by HybMap are presented for 12 (*isw1*Δ) and 14 (*ioc3*Δ) genes that appear down regulated in the single *rsc2* mutant (black bars) and suppressed in the double mutants (red bars).

Figure 5 – Supplement 1. Nucleosome profiles from microarray and sequencing show strong correlation with each other and predicted occupancy.

(A) The mean nucleosome profiles for each of the six gene clusters derived in Figure 10 are shown using data derived from paired-end sequencing. (B) The predicted mean nucleosome profile (Segal et al. 2006) is shown in orange along with the observed wild type nucleosome occupancy derived from microarray.

Figure 6 – Supplement 1. Wild type RNA expression levels are not significantly different between the six clusters.

(A) A histogram displays the representation of genes from each cluster on the custom mini-HybMap microarray. Cluster 6 is over-represented because of higher levels of RSC occupancy at these genes. (B) A box and whisker plot representing the distribution of median log2 coverage from stranded RNA sequencing for genes in each cluster. Data is from (Parkhomchuk et al. 2009). (C) A box and whisker plot representing the distribution of median log2 coverage from unstranded RNA sequencing for genes in each cluster. Data is from (Nagalakshmi et al. 2008). (D) A box and whisker plot representing the distribution of median log2 coverage from stranded RNA microarray for genes in each cluster. Data is from (Xu et al. 2009).

Figure 6 – Supplement 2. Occupancy of RSC and ISW1a as measured by sequencing.

Enrichment profiles for each of the six gene clusters derived in Figure 5 are shown for RSC and ISW1a .The profile for each cluster is drawn in a different color. Values are log2 fold enrichments over input and collected in 20 bp windows flanking the TSS ±800 bp. Windows overlapping neighboring genes were excluded. The Rsc8 enrichment shows strong enrichment for the +1 nucleosome but not upstream locations, possibly due to altered protein configurations or low efficiency. The Sth1 enrichment shows strong enrichment at both -1 and +1 nucleosomes, as well as a broad upstream enrichment for cluster 6, similar to the Rsc8 microarray. The Ioc3 enrichment also shows a broad enrichment over the upstream region for cluster 6.

Supplementary File 1 – Table of Yeast Strains

List of yeast strains and their genotypes used in this study.

Supplementary File 2 – Table of Plasmids

List of plasmid names and their sources used in this study.

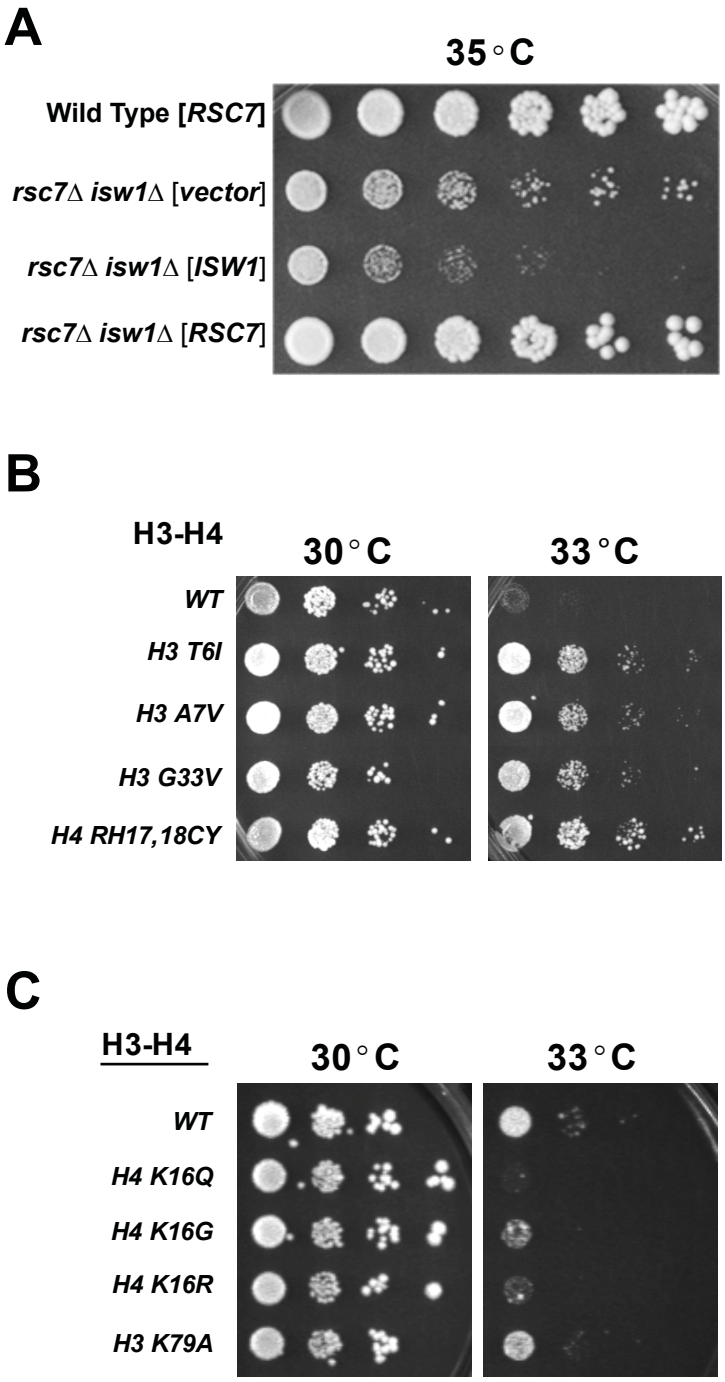
A
35°C
Wild Type [RSC7]
rsc7Δ isw1Δ [vector]
rsc7Δ isw1Δ [ISW1]
rsc7Δ isw1Δ [RSC7]
B
H3-H4
30°C
33°C
WT
H3 T6I
H3 A7V
H3 G33V
H4 RH17,18CY
C
H3-H4
30°C
33°C
WT
H4 K16Q
H4 K16G
H4 K16R
H3 K79A

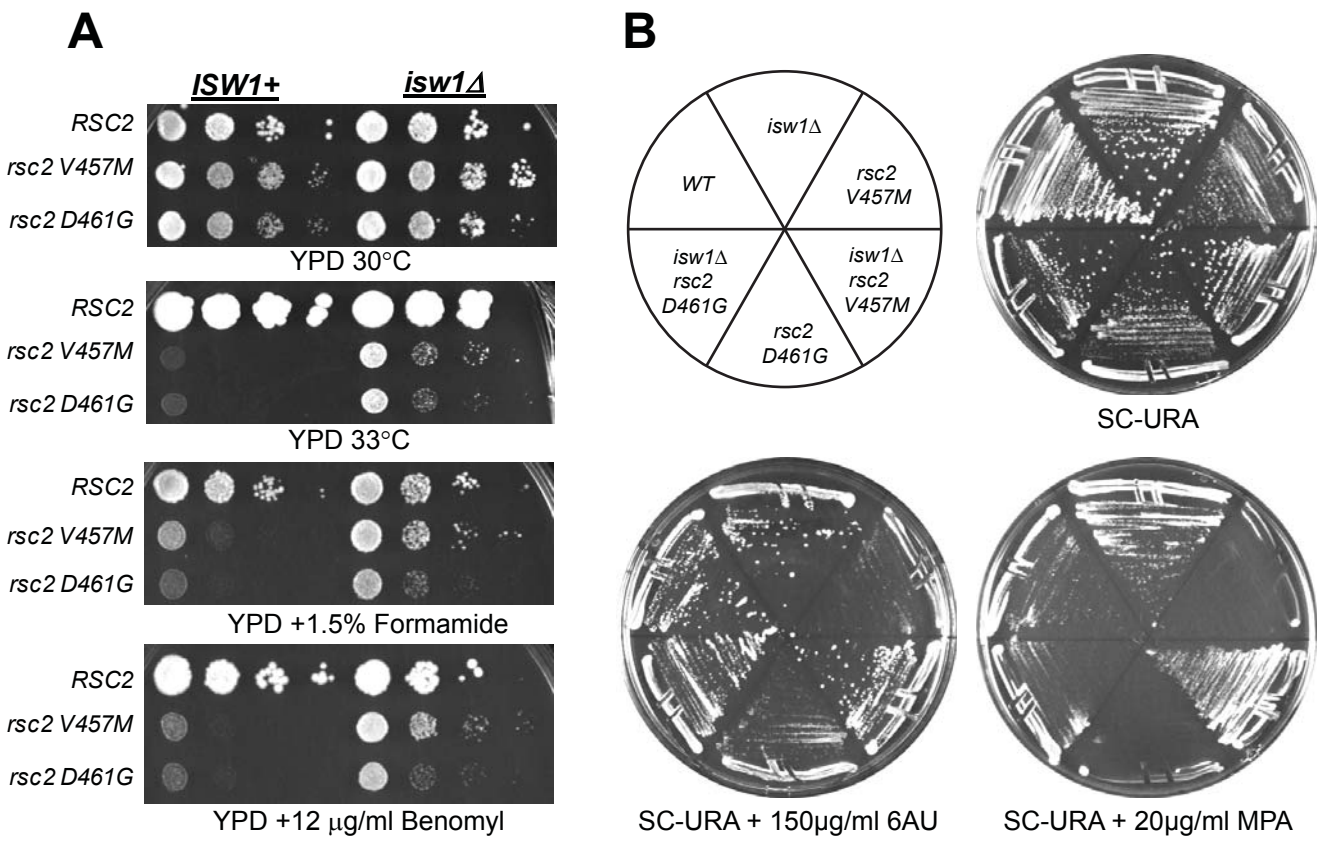
A
ISW1+
isw1Δ
RSC2
rsc2 V457M
rsc2 D461G
YPD 30°C
YPD 33°C
YPD +1.5% Formamide
YPD +12 μg/ml Benomyl
B
WT
isw1Δ
rsc2 V457M
isw1Δ rsc2 D461G
rsc2 D461G
isw1Δ rsc2 V457M
SC-URA
SC-URA + 150μg/ml 6AU
SC-URA + 20μg/ml MPA

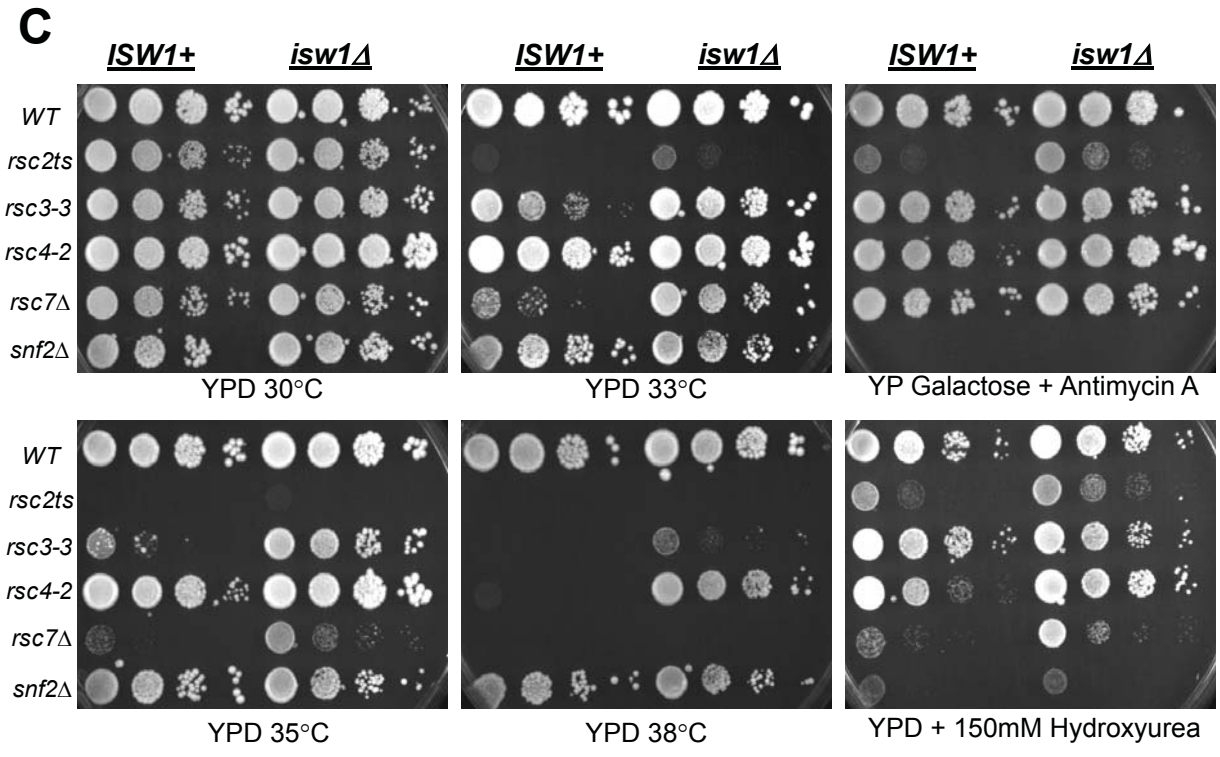
C
ISW1+
isw1Δ
WT
rsc2ts
rsc3-3
rsc4-2
rsc7Δ
snf2Δ
YPD 30°C
YPD 33°C
YP Galactose + Antimycin A
YPD 35°C
YPD 38°C
YPD + 150mM Hydroxyurea

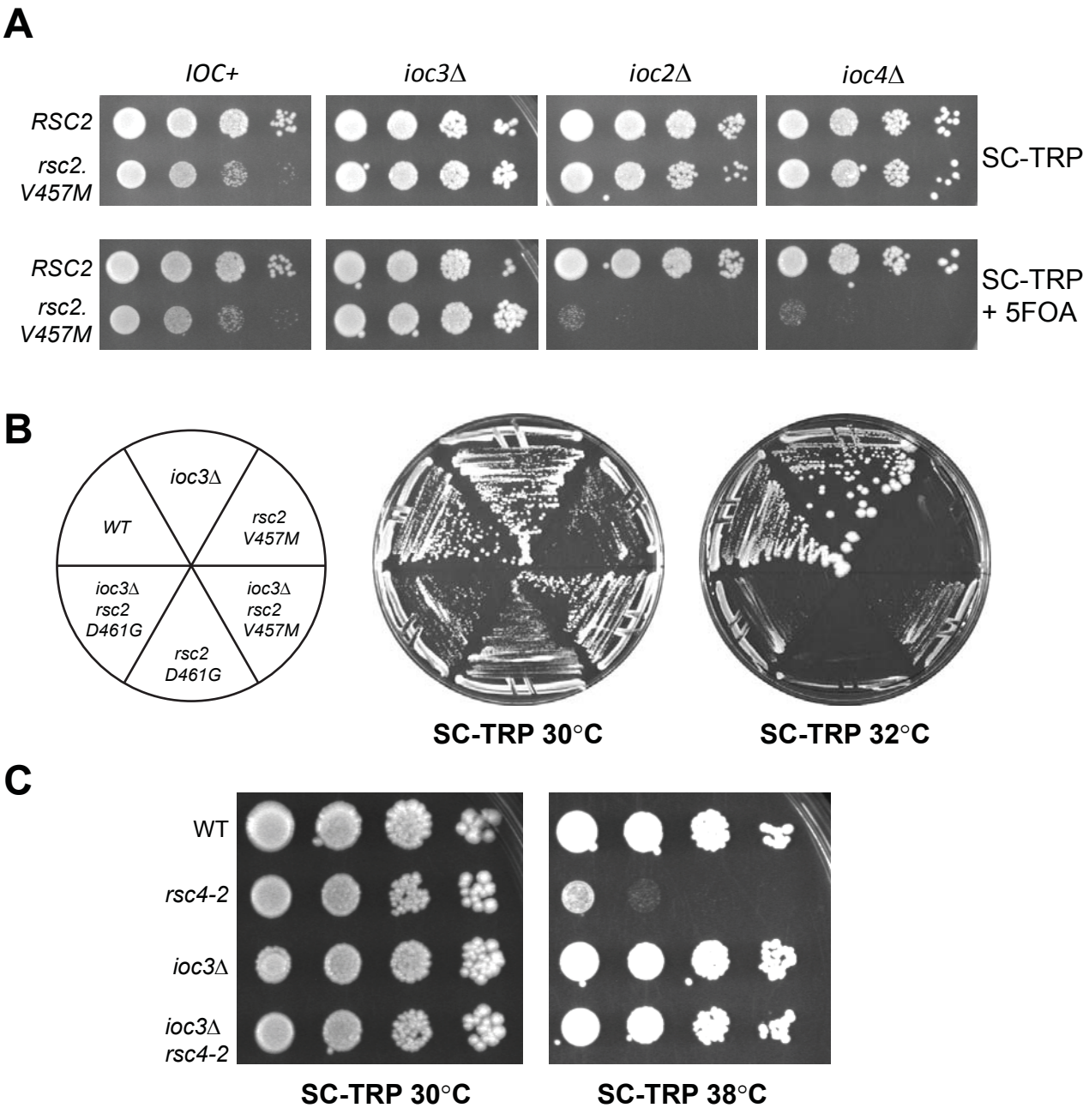
A
IOC+
ioc3Δ
ioc2Δ
ioc4Δ
RSC2
rsc2.
V457M
SC-TRP
RSC2
rsc2.
V457M
SC-TRP
+ 5FOA
B
ioc3Δ
rsc2
V457M
ioc3Δ
rsc2
D461G
rsc2
D461G
ioc3Δ
rsc2
V457M
WT
SC-TRP 30°C
SC-TRP 32°C
C
WT
rsc4-2
ioc3Δ
ioc3Δ
rsc4-2
SC-TRP 30°C
SC-TRP 38°C

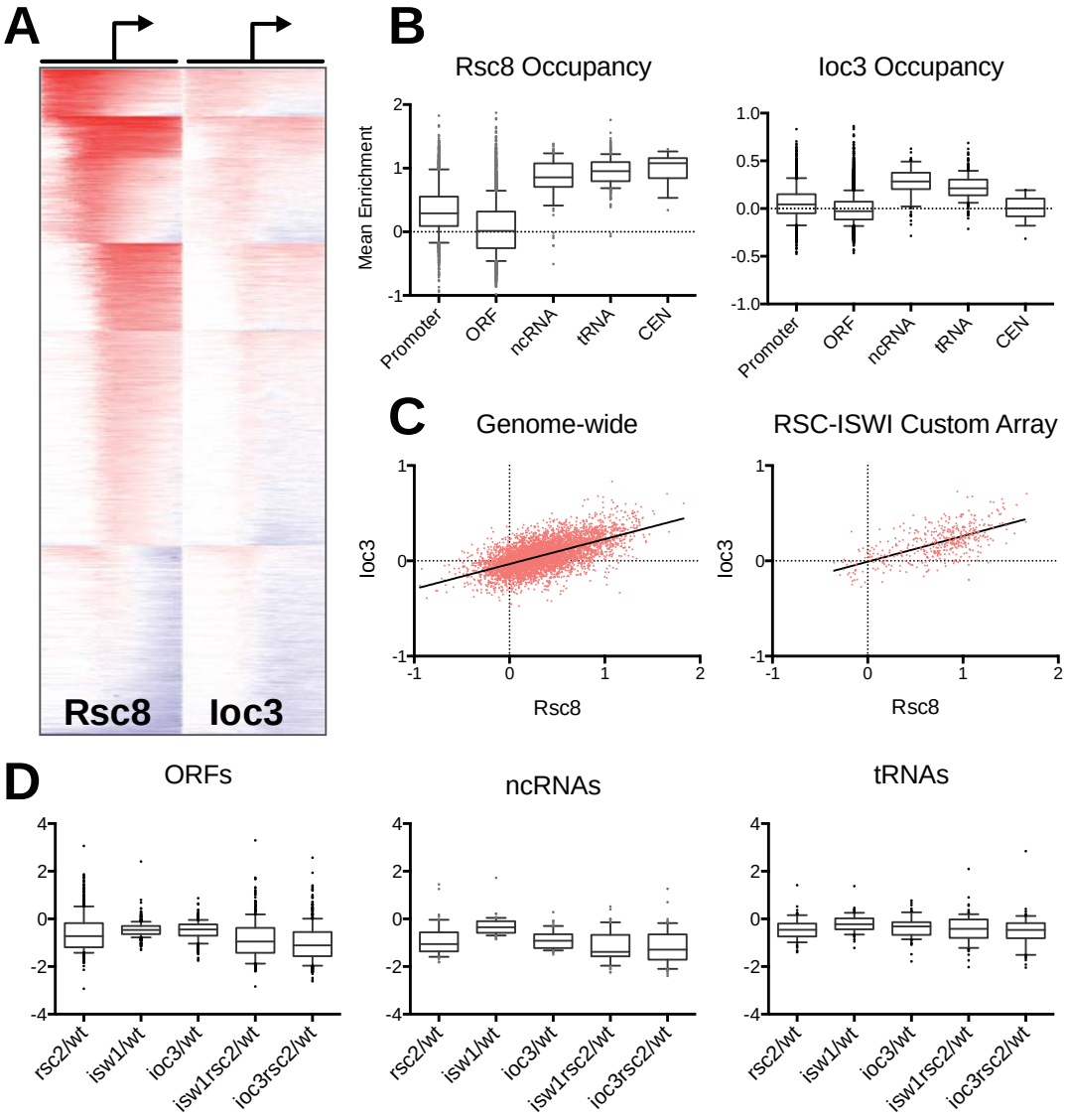
A
Rsc8
Ioc3
B
Rsc8 Occupancy
Ioc3 Occupancy
Mean Enrichment
Promoter
ORF
ncRNA
tRNA
CEN
C
Genome-wide
RSC-ISWI Custom Array
Ioc3
Rsc8
D
ORFs
ncRNAs
tRNAs
rsc2/wt
isw1/wt
ioc3/wt
isw1rsc2/wt
ioc3rsc2/wt

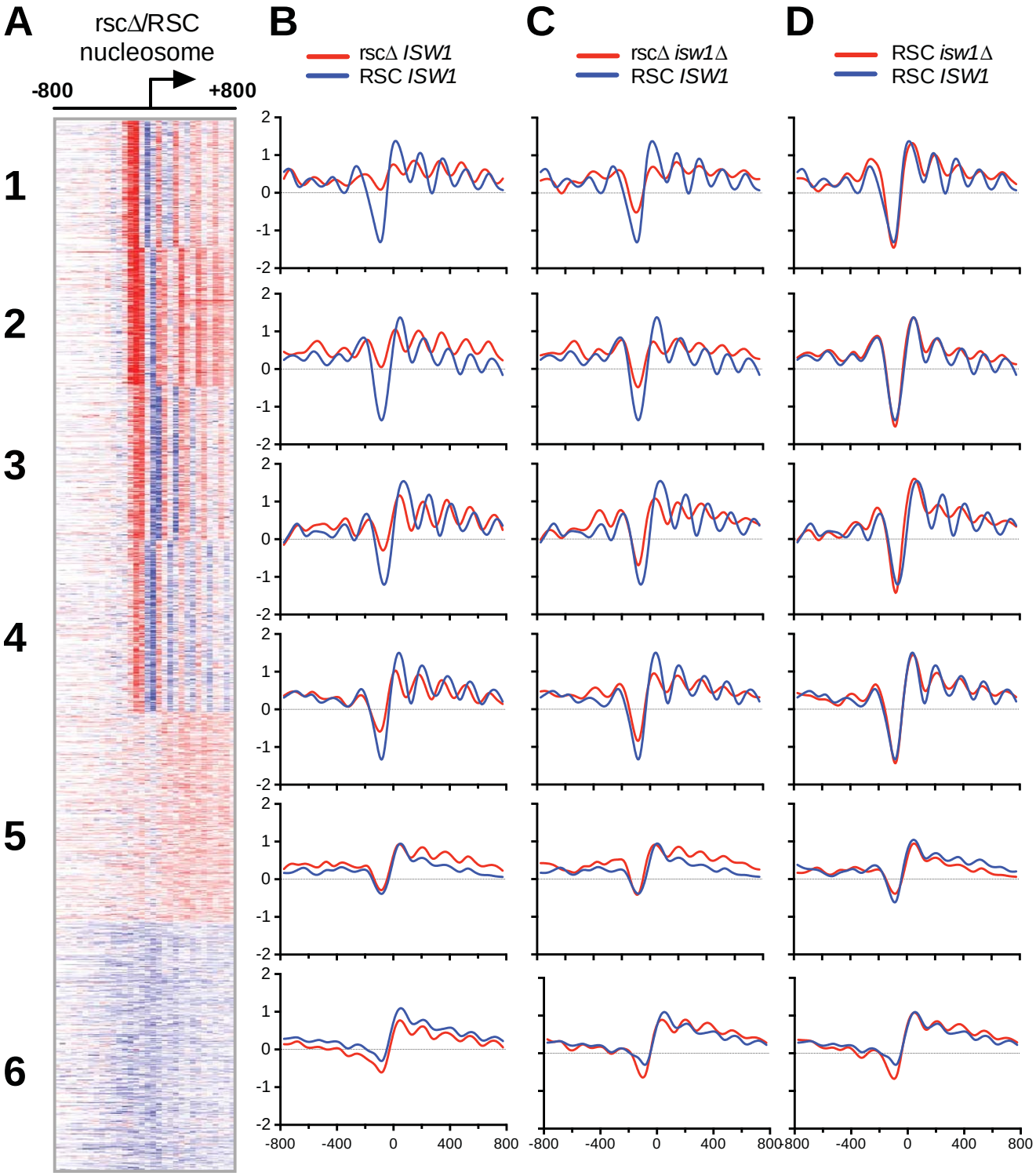
A
rscΔ/RSC
nucleosome
-800
+800
1
2
3
4
5
6
B
rscΔ ISW1
RSC ISW1
C
rscΔ isw1Δ
RSC ISW1
D
RSC isw1Δ
RSC ISW1
2
1
0
-1
-2
-800
-400
0
400
800

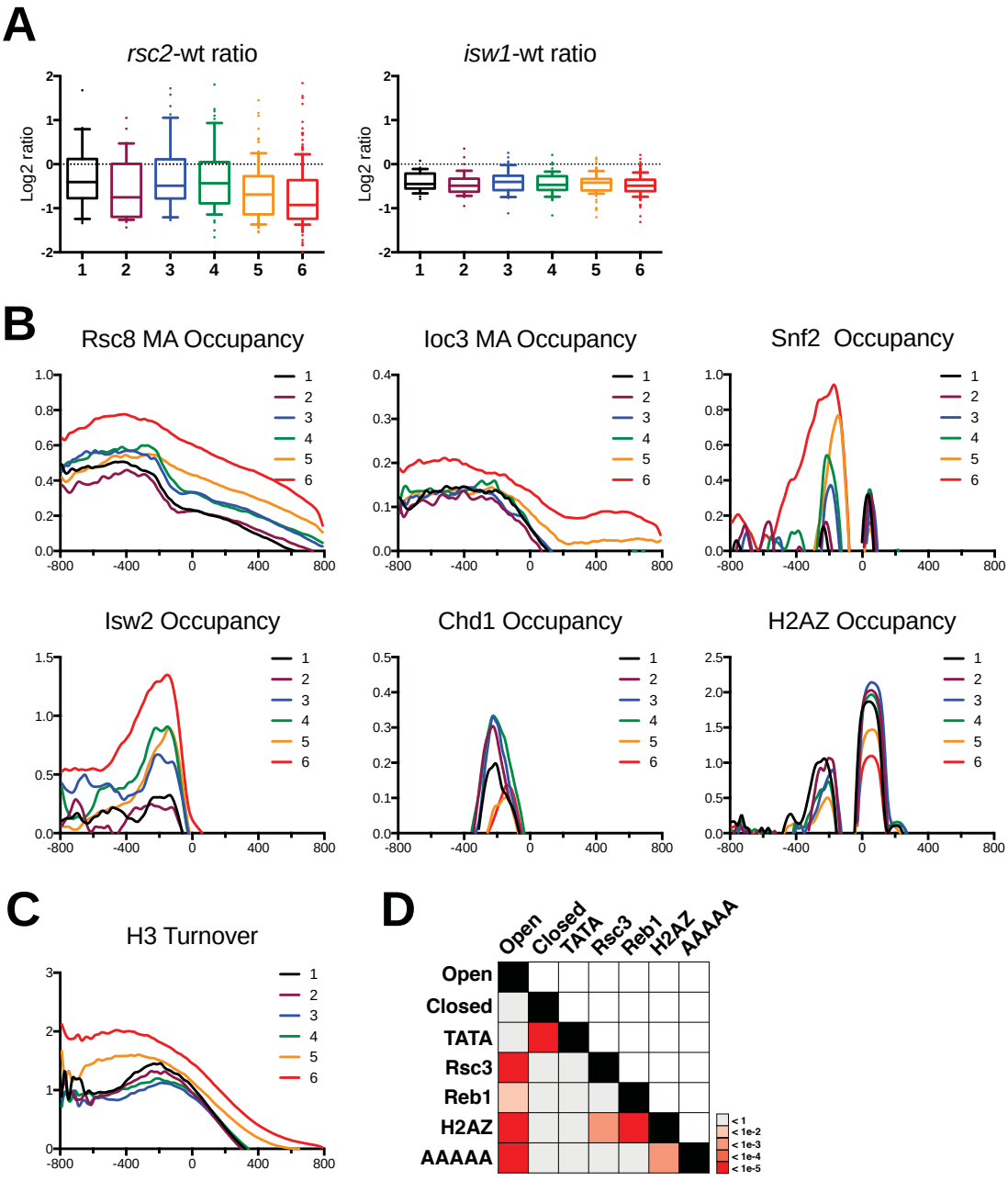
A
rsc2-wt ratio
isw1-wt ratio
Log2 ratio
B
Rsc8 MA Occupancy
Ioc3 MA Occupancy
Snf2 Occupancy
Isw2 Occupancy
Chd1 Occupancy
H2AZ Occupancy
C
H3 Turnover
D
Open
Closed
TATA
Rsc3
Reb1
H2AZ
AAAAA
< 1
< 1e-2
< 1e-3
< 1e-4
< 1e-5

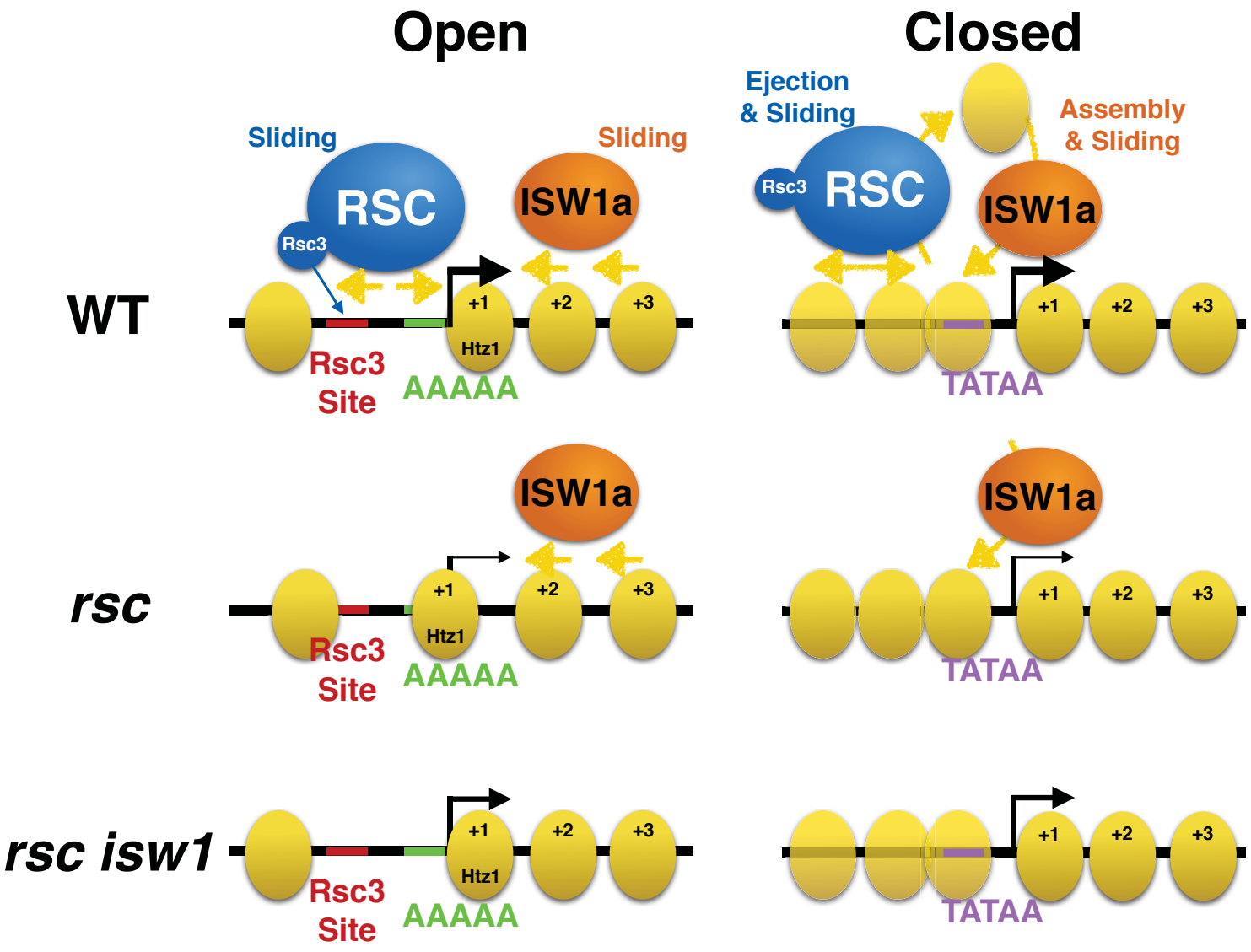
Open
Closed
WT
rsc
rsc isw1
Sliding
Sliding
RSC
Rsc3
ISW1a
Ejection
& Sliding
Assembly
& Sliding
+1
+2
+3
Htz1
Rsc3
Site
AAAAA
TATAA